Lecture 3-5
Instrumentation

Requirements

1. Vacuum

- Mean Free Path
- Contamination
- Sticking probability

UHV

- Materials
- Strength
- Stability
- Permeation

Design considerations

- Pumping speed
- Virtual leaks
- Leaking
- de-greasing

Vacuum pumps

- Diffusion
- Ion pumps
- Turbo molecular pumps
- Sublimation pumps
- Cryo pumps

2. Sample handling

- Preparation
- Treatment in vacuum
- Manipulation

Instrument : Light source, analyser, detector

Resolution, Sensitivity

Width of radiation
Width of the level
Analyser resolution

FW HM

Analysers

Dispersive

Retarding potential

Photon Intensity

$I_{(Photoelectrons\ at\ detector)}$ σ, I_{nr}, A_S, α → Analyser solid angle

σ → Cross section

A_S → Area of the slit

Transmission → Fraction of electrons reaching the detector from an isotropic point source

= Useful instrument solid angle . Transmission factor

Integral of point source transmission over slit area → luminority

Integral of solid angle over slit area → étendue

Line width of radiation → pressure broadening
(Stark, van der Waals, resonance)

Doppler broadening
Recoil of atoms
Life time

$I(\theta) = 1 + \beta/2\,[3/2\,(\sin^2\theta) - 1]$ for unpolarised photons

β- asymmetry parameter

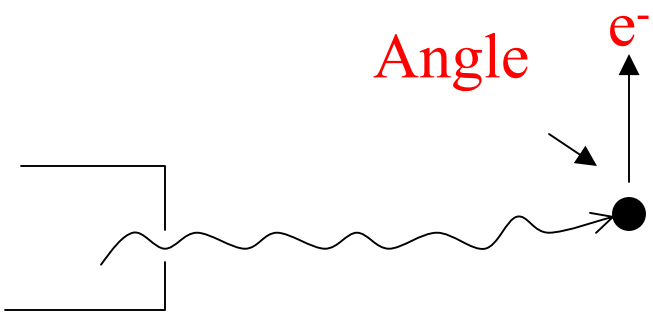

Surface Sensitivity

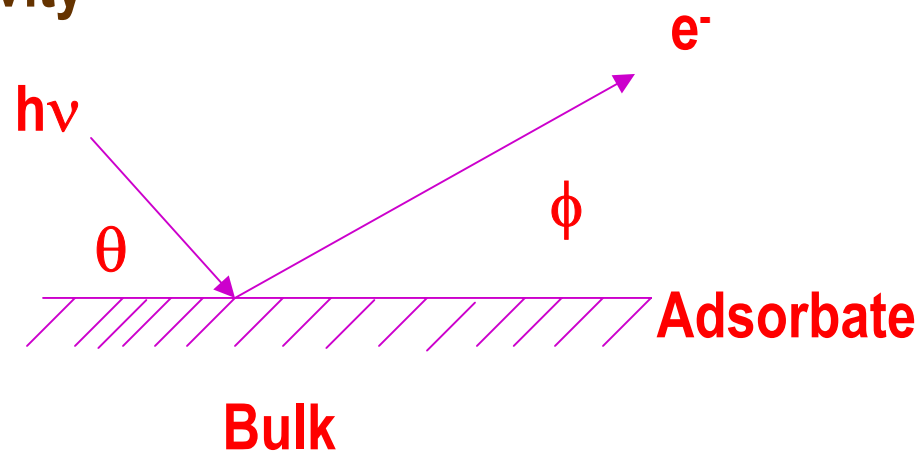

Other techniques

Photo detachment
EXAFS, SEXAPS, synchrotron radiation

EPMA or Electron probe x-ray micro analysis

Ion beam techniques

SIMS
- dynamic
- static

ISS
RBS
FABMS

INS (ion neutralization spectroscopy)

SNMS (sputtered neutral mass spectrometry)
PIXE (particle induced x-ray emission

History

Photoelectric effect 1887 Hertz

Rutherford β ray spectroscopy Before WWI

Basic XPS equation, $E_K = h\nu - E_B$ Originally stated by Rutherford 1914

Moseley After WWI

Rawlinson

Robinson β ray spectrum of elements

Anomalous lines corresponding to electron ejection due to fluorescence excitation.

Anger spectroscopy 1925

Steinhardt 1951

"An x-ray photoelectron spectrometer for chemical analysis"

Kai Seigbahn – Uppsala 1940's
1967 "ESCA: Atomic, Molecular and solid state structure studied by means of Electron spectroscopy"

Acronym ESCA is due to Seigbahn

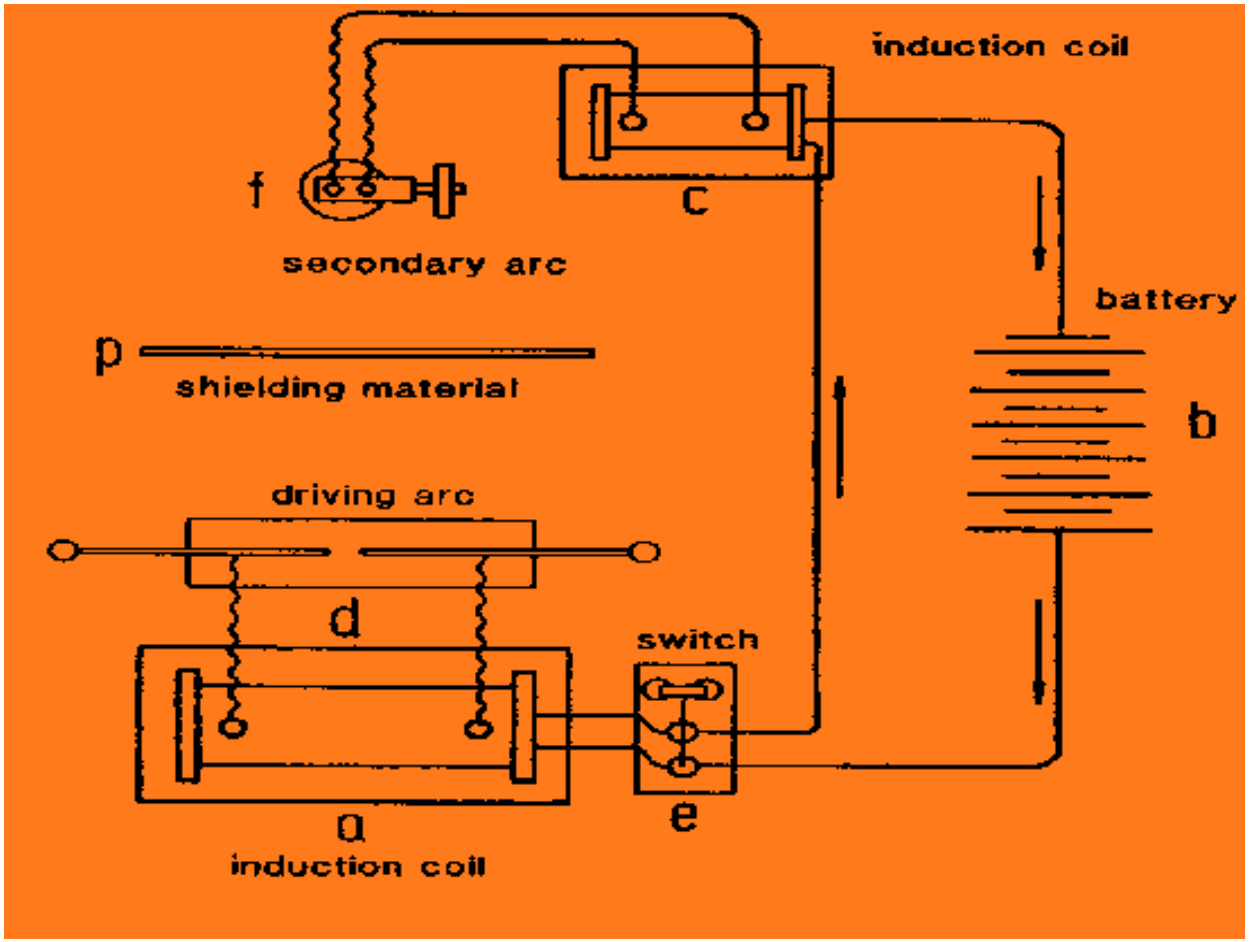

Early Hertz Experiment

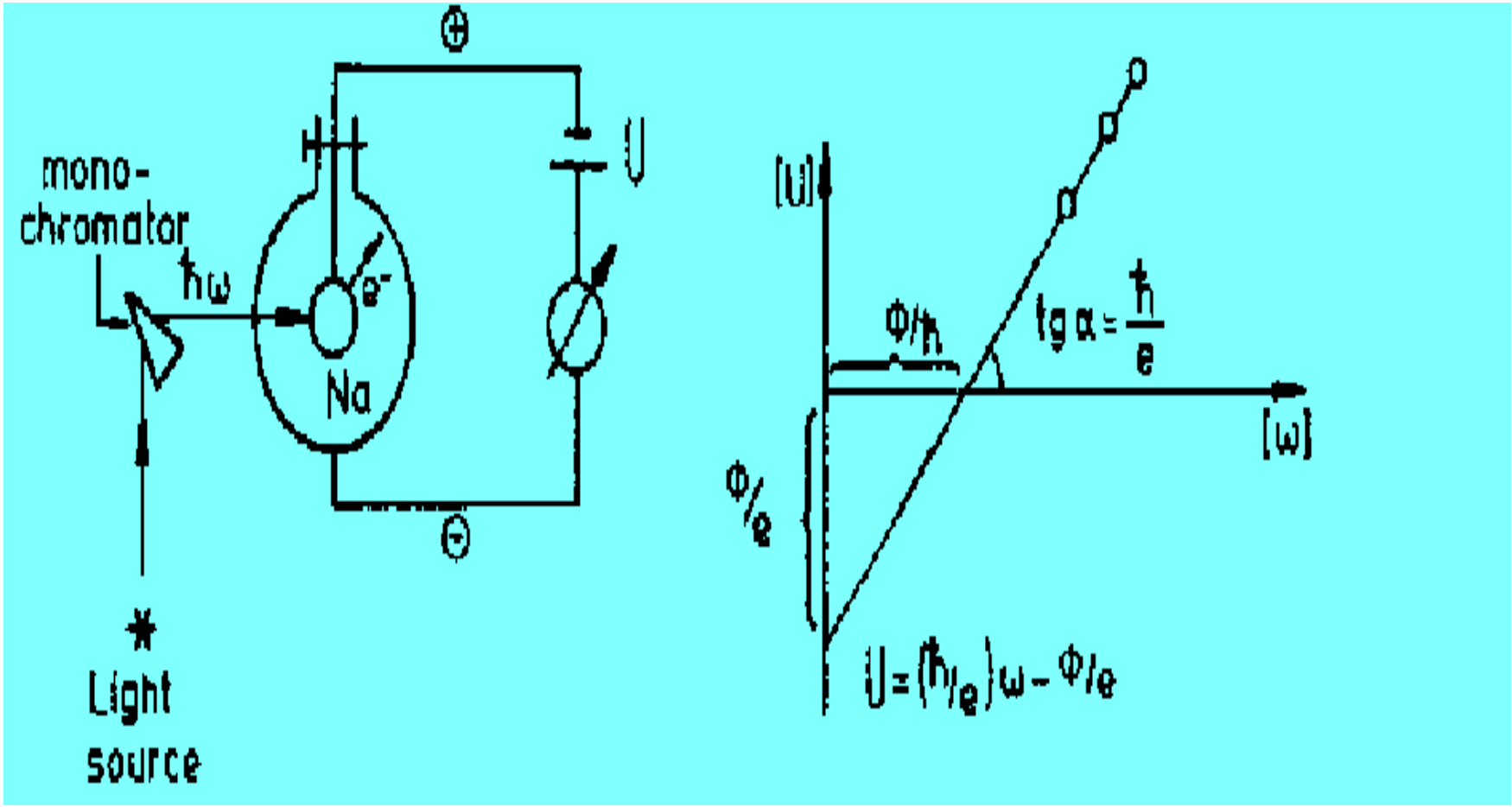
mono-
chromator
hω
e⁻
Na
U
Light
source
[U]
Φ/h
tg α = h/e
[ω]
Φ/e
U = (h/e)ω - Φ/e

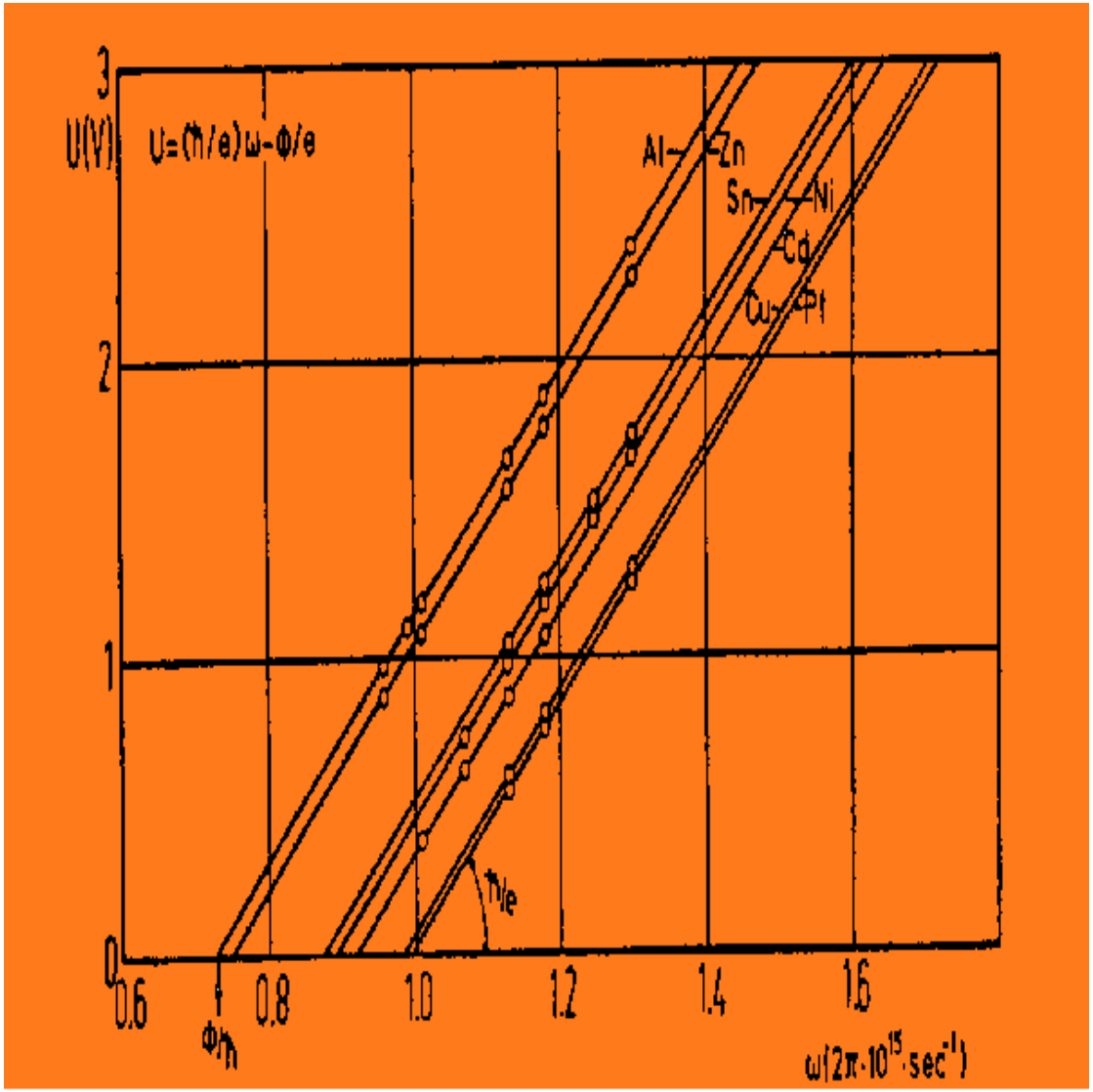

U vs. ω for a number of metals

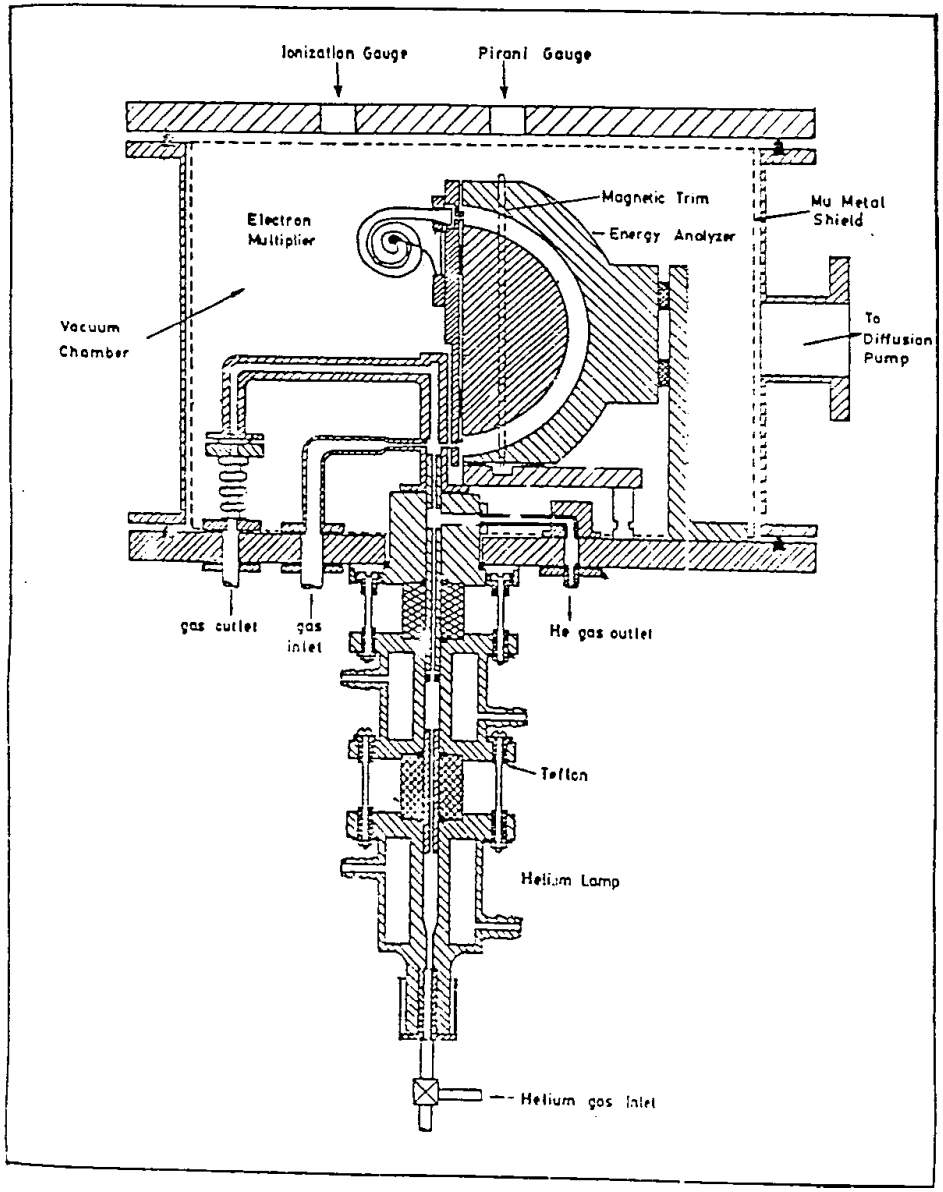
Ionization Gauge
Pirani Gauge
Magnetic Trim
Mu Metal Shield
Energy Analyzer
Electron Multiplier
Vacuum Chamber
To Diffusion Pump
gas outlet
gas inlet
He gas outlet
Teflon
Helium Lamp
Helium gas inlet

Simple UPS

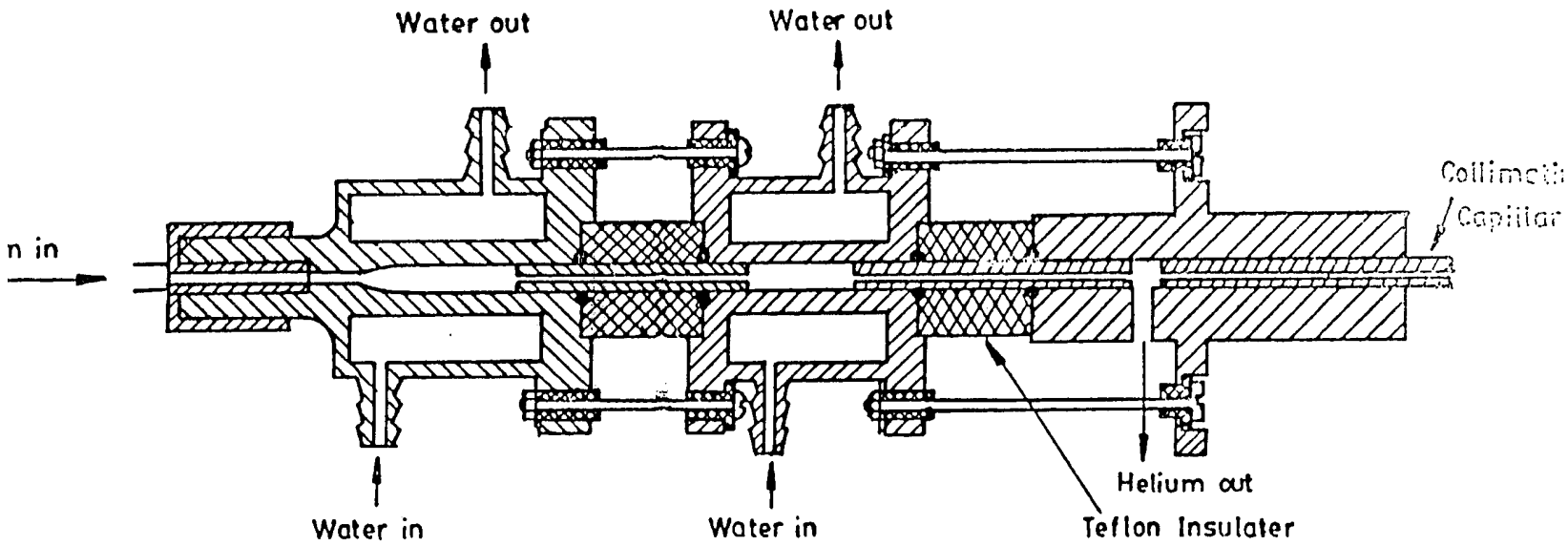

Fig. I.5. Cross-sectional view of the helium discharge lamp.

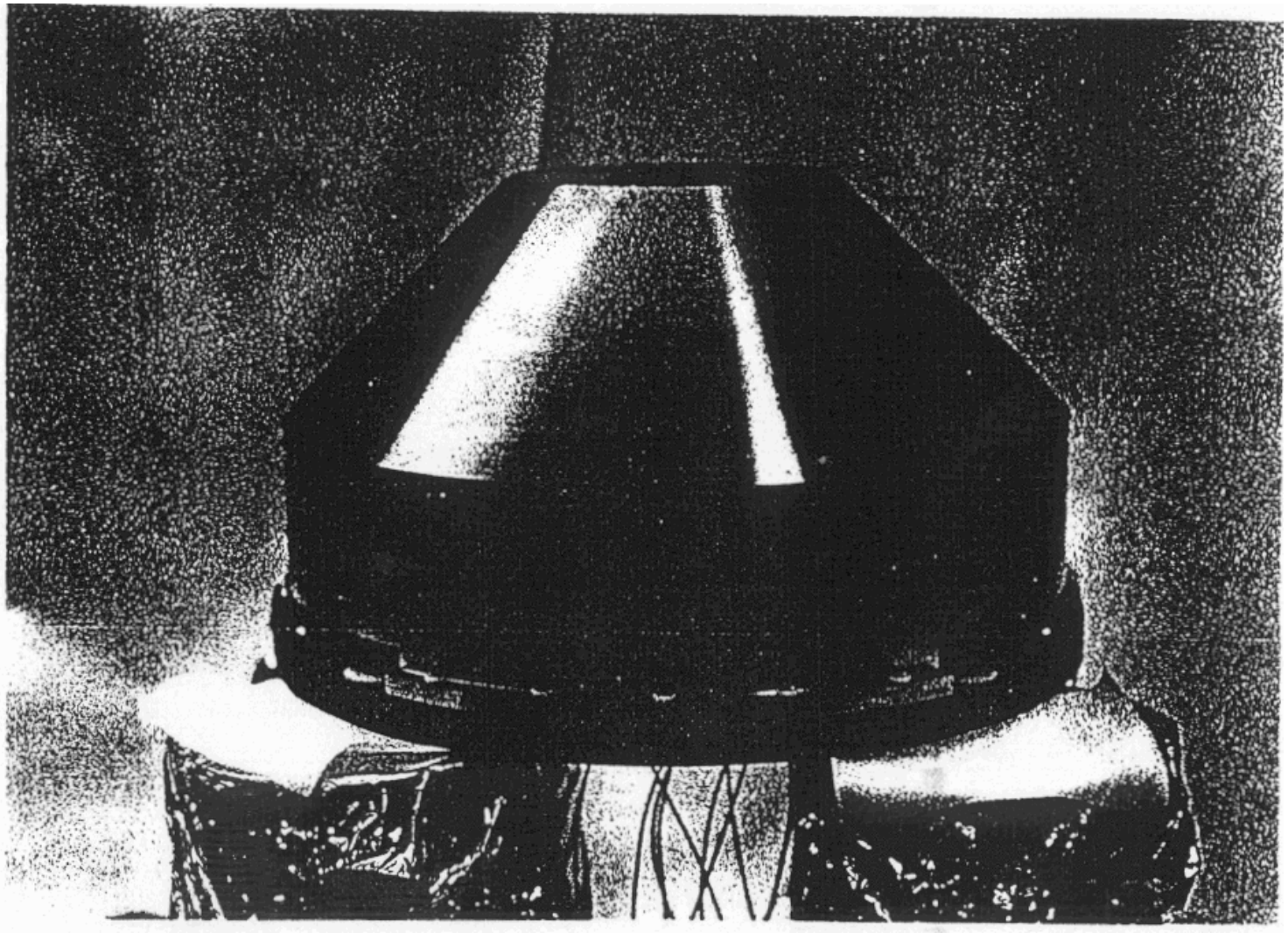

Heart of the instrument

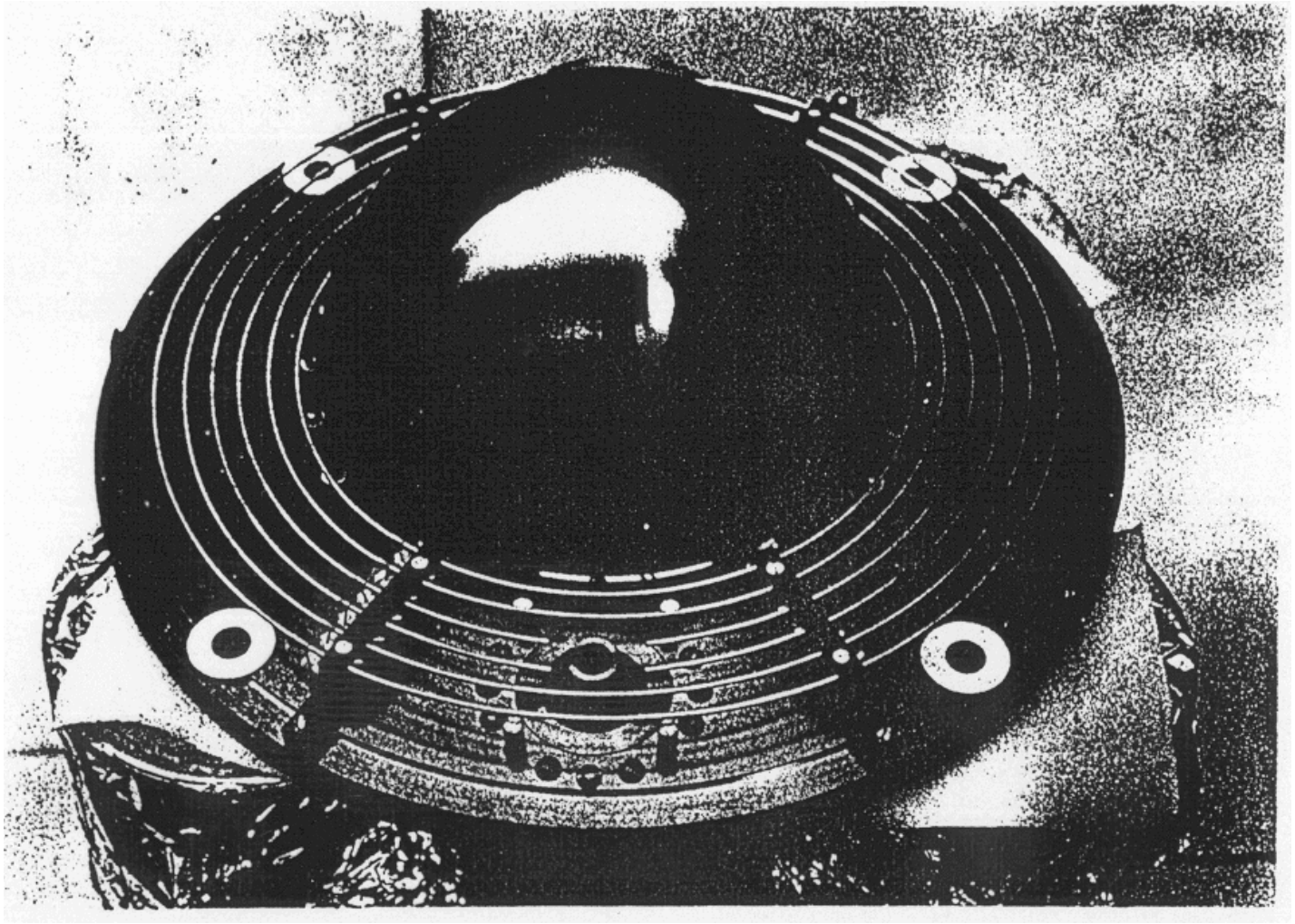

What is inside

X-Ray Source

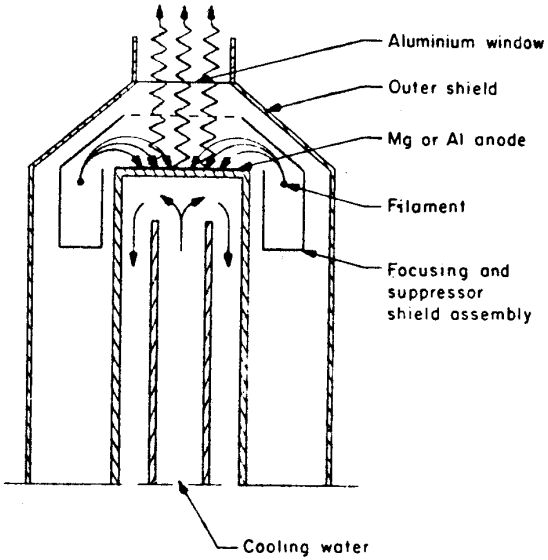

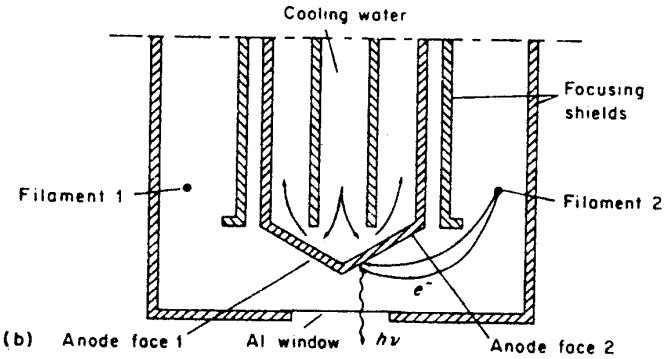

Figure 2.9 (a) Soft X-ray source with single anode of either magnesium o aluminium, deposited as a thick film on the flat end of a water-cooled copper bloc The anode is surrounded by a cylindrical focusing shield at the same potential as th filament. An outer can acts as a radiation shield and carries the thin aluminiu window that must be interposed between the target and sample. (Reproduced b permission of Perkin-Elmer, Physical Electronics Division) (b) Soft X-ray source wit dual anode, allowing use of either magnesium or aluminium $K\alpha$ radiation by simp external switching without the need to break the vacuum in going from one to th other. The anode has a tapered end with two inclined faces on which films of mag nesium and aluminium, respectively, are deposited. There are two semi-circular fil ments, one for each face. The focusing arrangements are similar to those for the singl anode of (a). (Reproduced from Barrie and Street[18] by permission of The Institute o

X-Ray emission spectrum

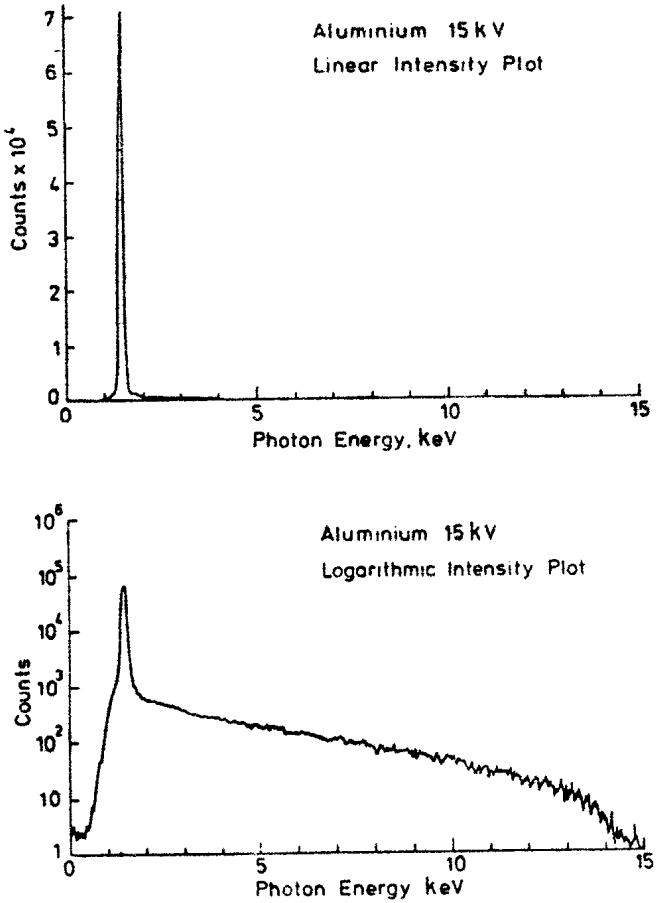

Figure 2.11 X-ray emission spectrum of an aluminium target under bombardment by 15 kV electrons, recorded by a lithium-drift detector through a beryllium window of thickness 7.5 μm. Upper curve, photon intensity plotted on a linear scale, on which little is evident except the intense characteristic $K\alpha$ line. Note that the energy broadening of the solid-state detector attenuates the peak by a factor of about 100. Lower curve, the same plotted on a logarithmic scale, that reveals more clearly the broad Bremsstrahlung background extending to energies much higher than the characteristic line. The background intensity at very low energies will have been reduced by absorption in the beryllium window. (Measurements by courtesy of Mr R. W. M. Hawes, Materials Development Division, Harwell)

Detail of the spectrum

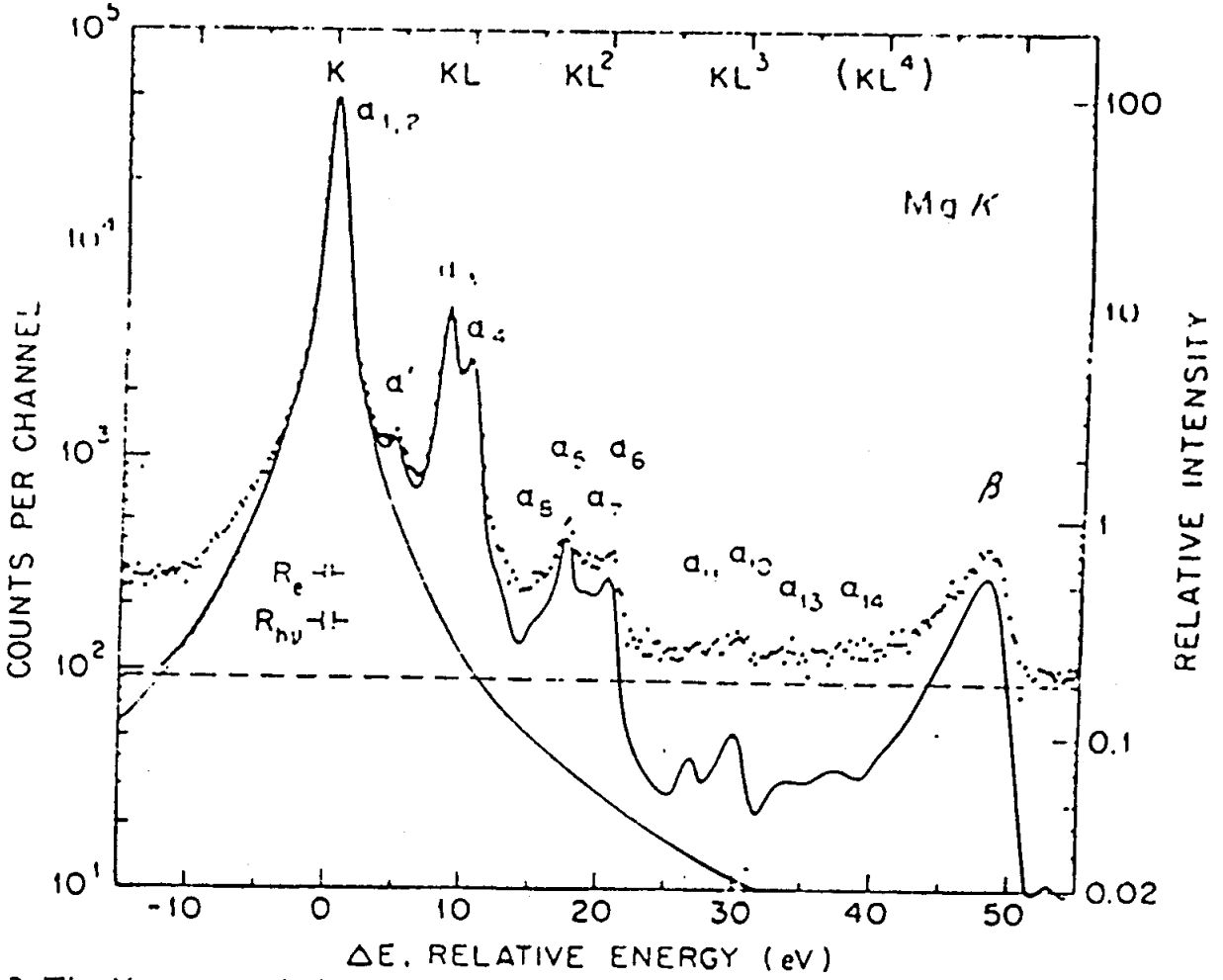

Fig. 2. The K x-ray emission spectrum of Mg metal as emitted by a non-monochromatized x-ray source. The peaks indicated $\alpha_1, \alpha_2, \ldots, \beta$ correspond to various transitions into the K = 1*s* subshell. The dashed line is an average background and the solid line is the net spectrum. Note the logarithmic intensity scale. The notation K corresponds to a single initial 1*s* hole, KL to initial holes in both 1*s* and 2*s* or 2*p*, KL^2 to a single initial hole in 1*s* and two initial holes in 2*s*, 2*p*, etc. (From Krause and Ferreira, ref. 37.)

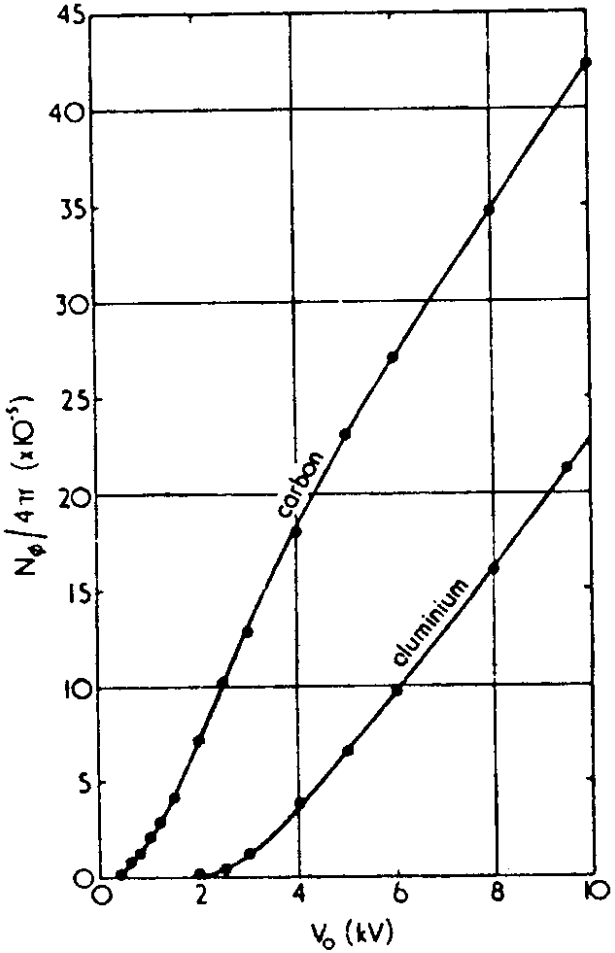

Figure 2.10 Dependence of efficiency of production of Al $K\alpha$ and C $K\alpha$ characteristic radiation on the energy of the bombarding electrons. (Reproduced from Dolby[20] by permission of The Institute of Physics)

Table 2.1 Energies and widths of some characteristic soft X-ray lines

Line	Energy, eV	Width, eV
Y $M\zeta$	132.3	0.47
Zr $M\zeta$	151.4	0.77
Nb $M\zeta$	171.4	1.21
Mo $M\zeta$	192.3	1.53
Ti $L\alpha$	395.3	3.0
Cr $L\alpha$	572.8	3.0
Ni $L\alpha$	851.5	2.5
Cu $L\alpha$	929.7	3.8
Mg $K\alpha$	1253.6	0.7
Al $K\alpha$	1486.6	0.85
Si $K\alpha$	1739.5	1.0
Y $L\alpha$	1922.6	1.5
Zr $L\alpha$	2042.4	1.7
Ti $K\alpha$	4510.0	2.0
Cr $K\alpha$	5417.0	2.1
Cu $K\alpha$	8048.0	2.6

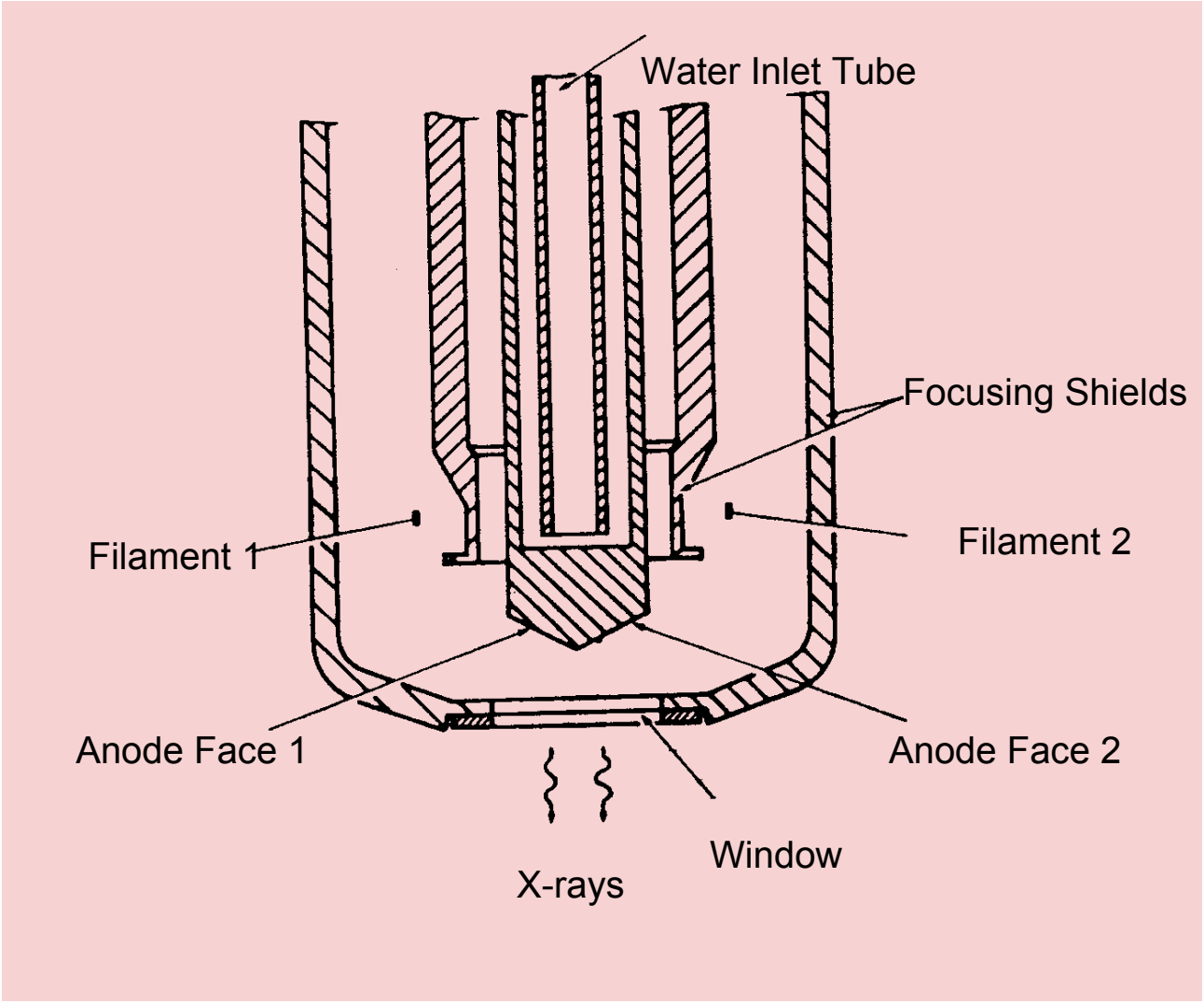

X-ray source with dual filament and anode faces

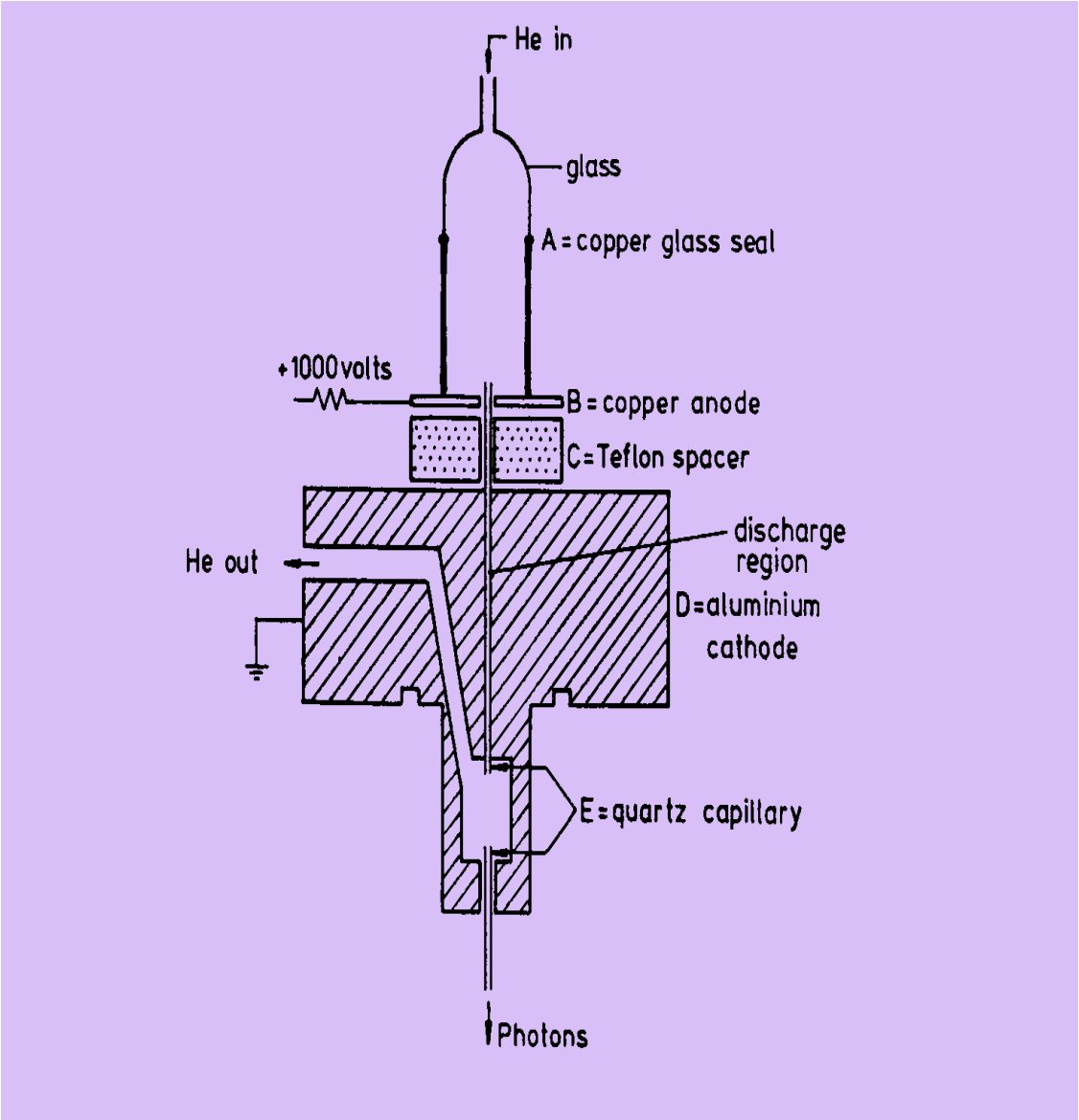
He in
glass
A = copper glass seal
+1000 volts
B = copper anode
C = Teflon spacer
He out
discharge region
D = aluminium cathode
E = quartz capillary
Photons

UV Source

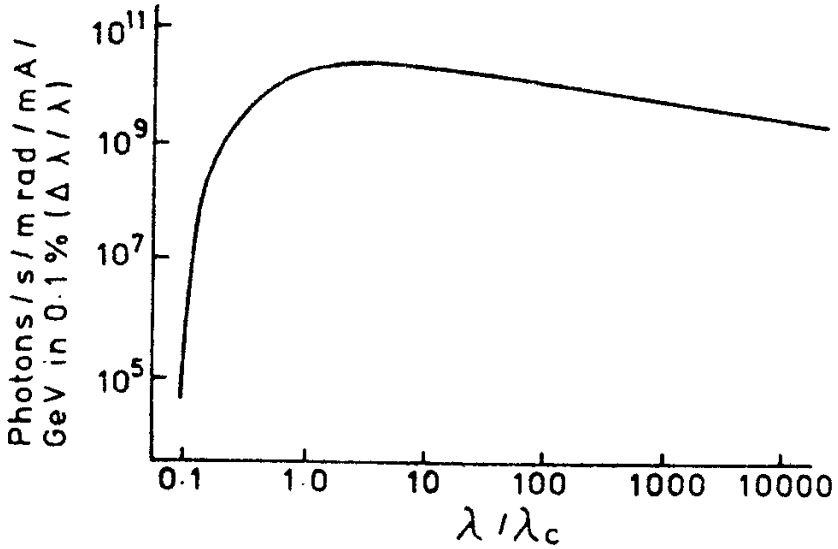

Figure 2.13 Shape of the radiation spectrum of an electron travelling in a curved orbit. The vertical scale of photon flux is a function only of the electron energy and current, while the horizontal scale is defined by λ_c, the so-called critical wavelength. If the maximum intensity is required to be at an energy near 1000 eV, then λ_c should be 1 °A or less. To achieve that the orbiting electrons must be accelerated to several gigaelectronvolts, and the radius of the orbit should be of the order of a few metres (After Farge and Duke[24])

Synchrotron

Resolution

Absolute resolution, FWHM ΔE

Base width $\Delta E_B = 2\,\Delta E$

Relative resolution $R = \Delta E/E_0$

Represented normally, in percentage, $\Delta E/E_0 \times 100$

Resolving power $\rho = 1/R = E_0/\Delta E$

XPS line widths 0.7eV Mg K_α, 0.85 eV Al K_α, Ffr an absolute resolution of 0.2 eV, the relative resolution is 10^{-4} or a resolving power of 10,000.

To keep the analyser size to an optimum value, the KEs have to be retarded - pass energy.

For an absolute resolution of 0.2 eV, the relative resolution is only 10^{-3}. High absolute resolution can be achieved by retardation.

Not always advantageous.

Requirement in UPS

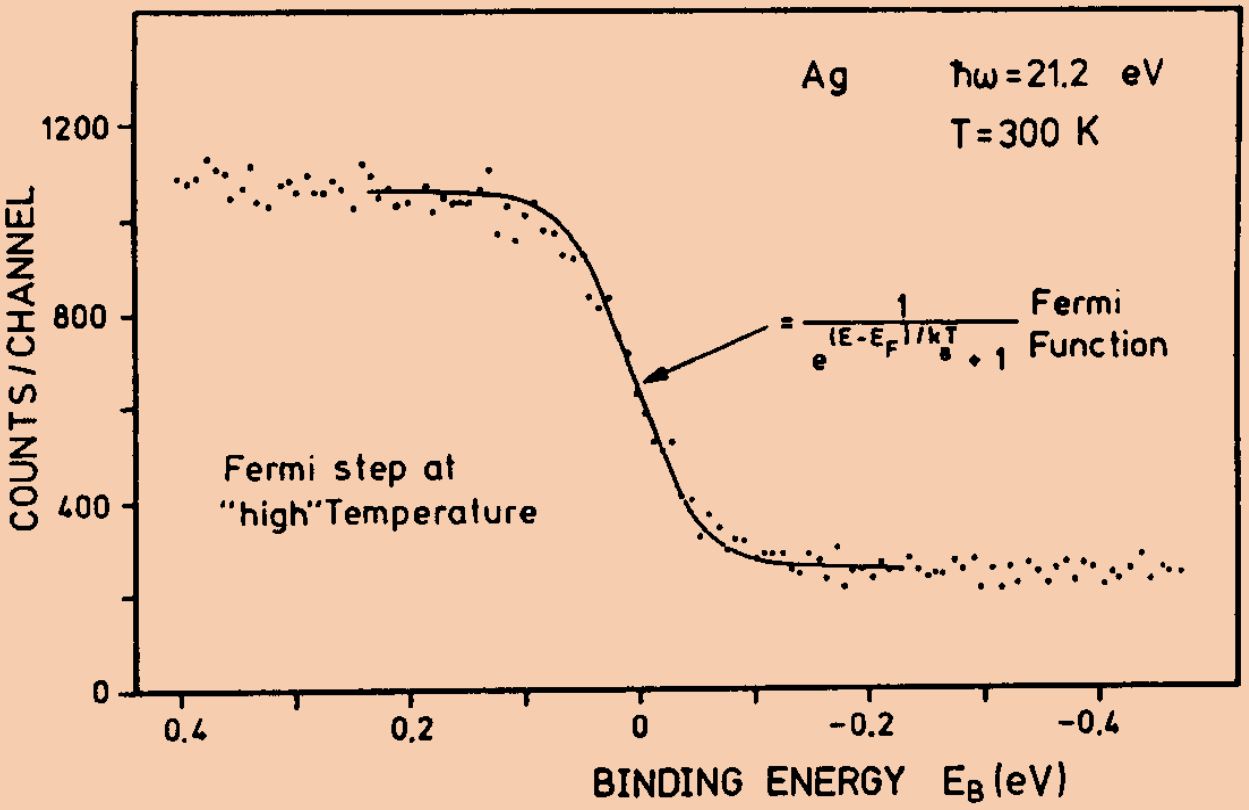

EDC around E_F in an UPS spectrum of Ag. Solid line is the Fermi function at RT

Electronic structure of solids

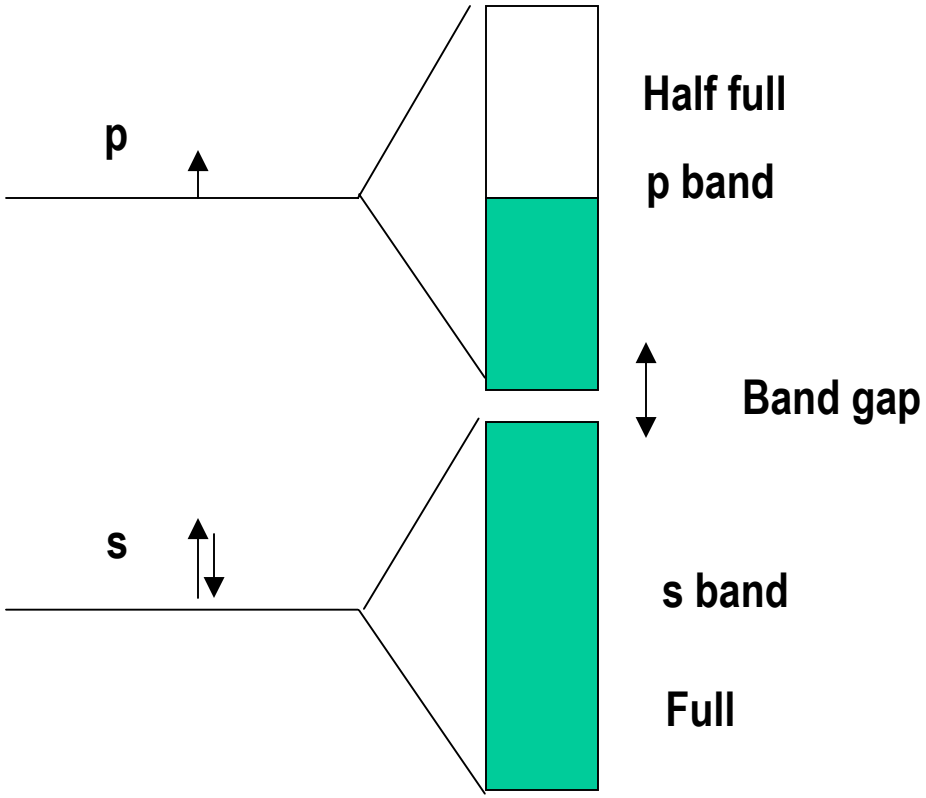

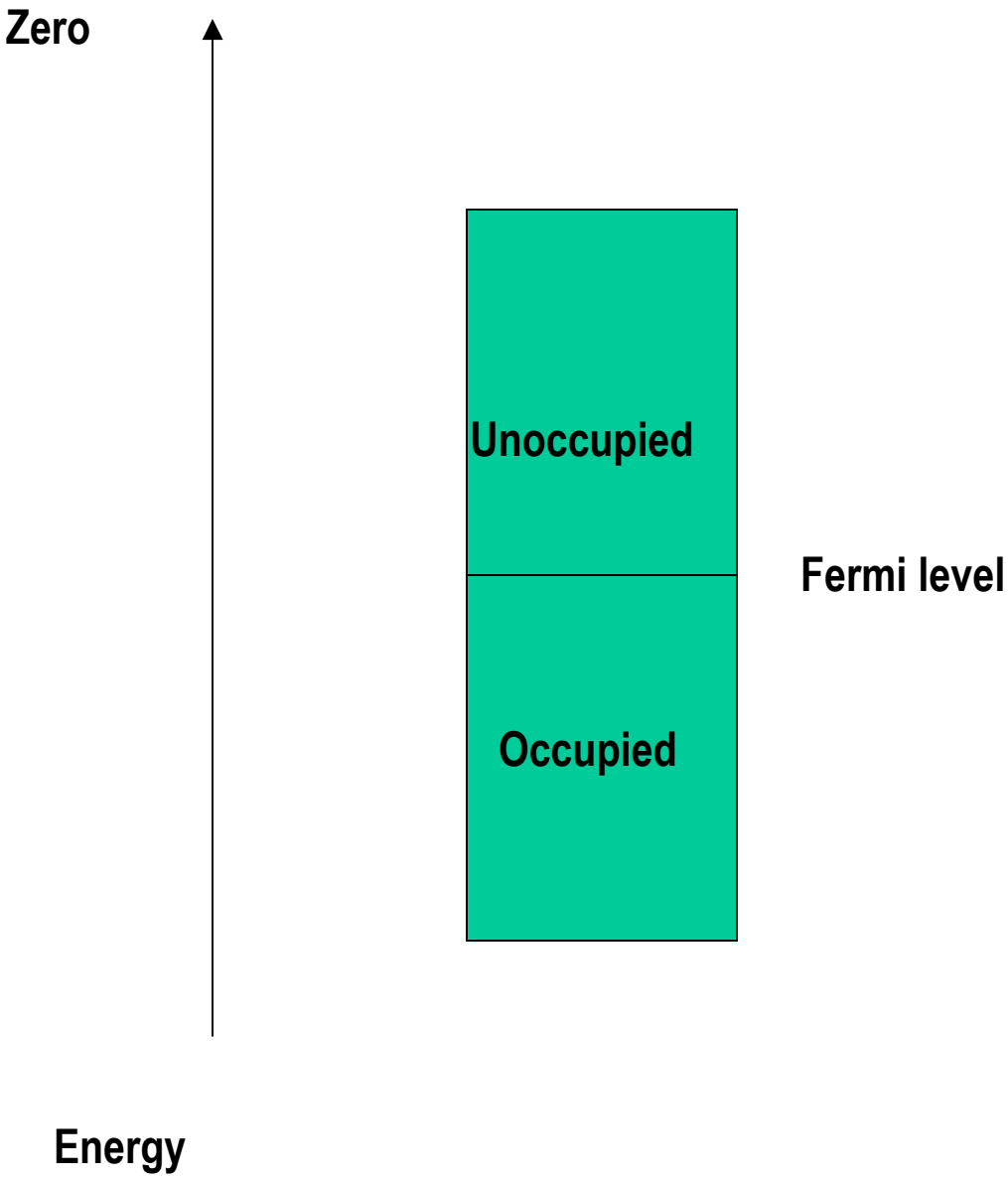
Zero
Unoccupied
Fermi level
Occupied
Energy

In a piece of metal, there are 10^{23} electrons.
We have high quantum states for most electrons.

Probability that a given quantum state is occupied is given by the **Fermi factor,**

$$f(E) = 1/[e^{(E-\mu)/kT} + 1]$$

Plot of this is given here which gives a definition of Femi level.

μ is chemical potential, is the energy of the level for which f(E) = ½

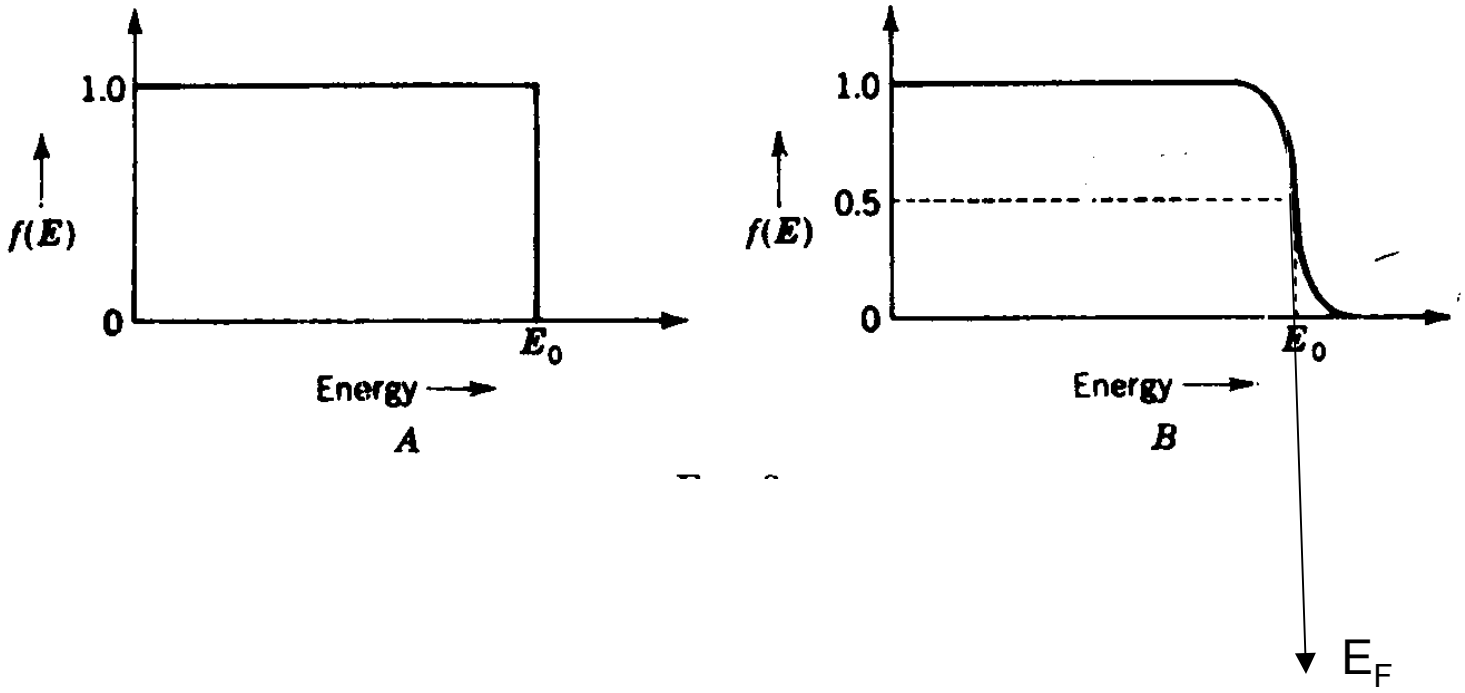

How the given energy states are occupied at a given temperature is given by Fermi-Dirac distribution.

$$N(E)dE = f(E)S(E)dE$$
$$= S(E)dE/e^{(E-\mu)/kT} + 1]$$

N(E) = number of electrons per unit volume, having energy between E and E + dE
S(E) = number of available quantum states in this energy range.

This distribution obeys Pauli exclusion principle.
Number of electrons N(E) can never be larger than the number of available states S(E) as the denominator is always greater than one.

For states with energies well above μ, 1 in the denominator can be neglected.
$N(E)dE \approx e^{-(E-\mu)/kT}$ This resembles Bolzmann distribution

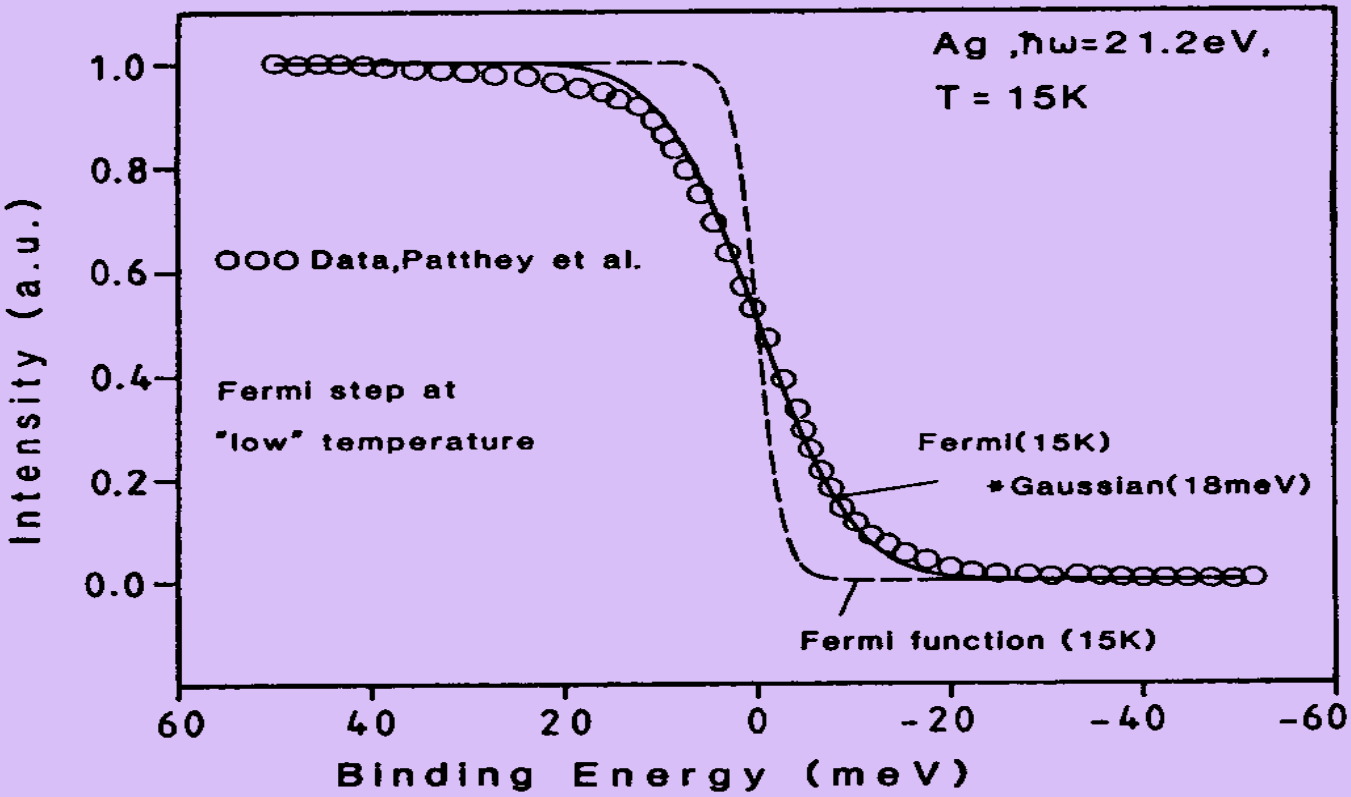

UPS EDC at E_F of Ag (15 K). Resolution, ΔE is obtained by convoluting a Fermi function with a Gaussian function

Analysers

Retarding Field Analyser

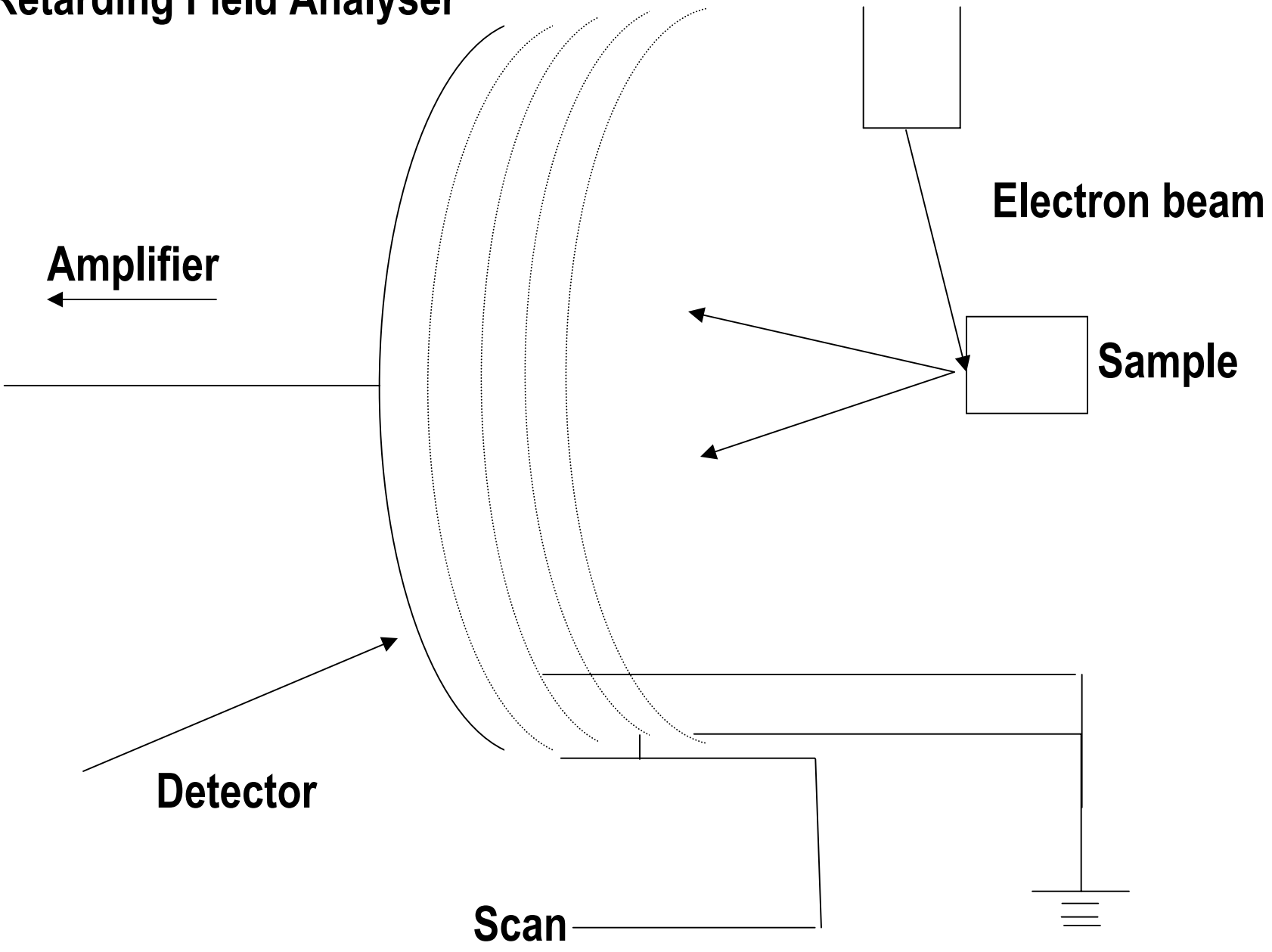

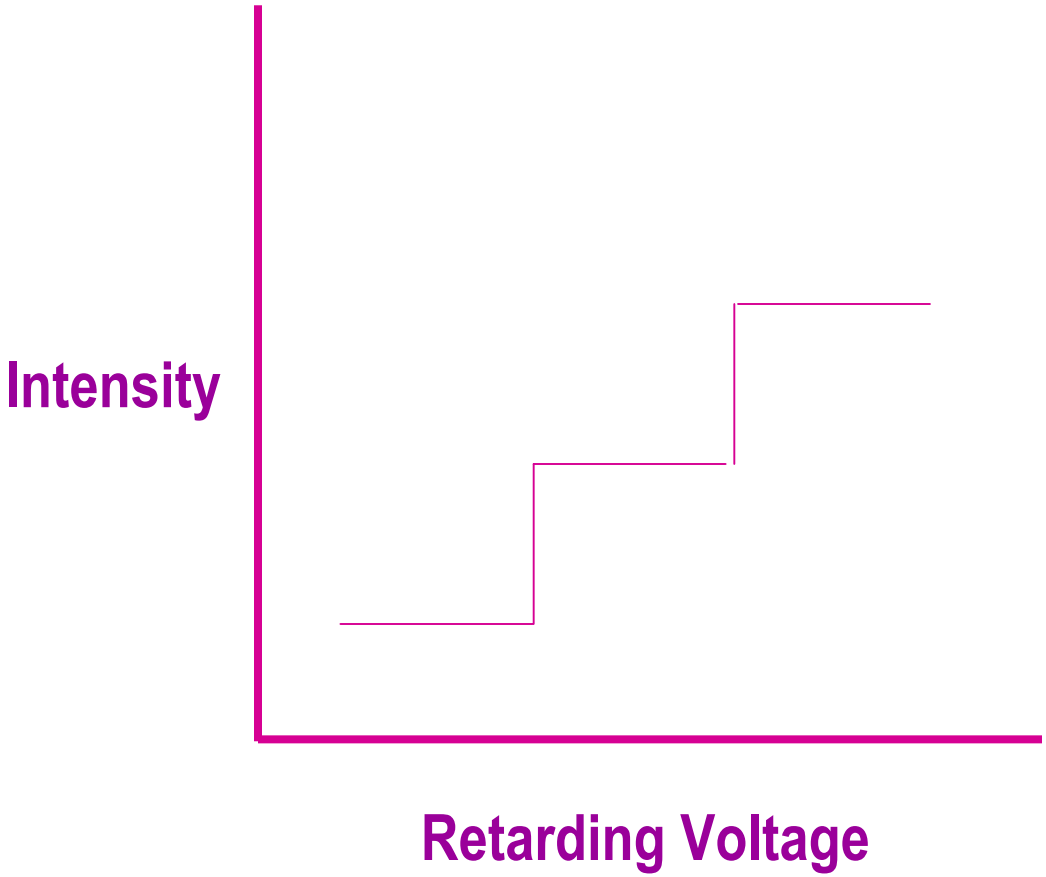
Intensity
Retarding Voltage

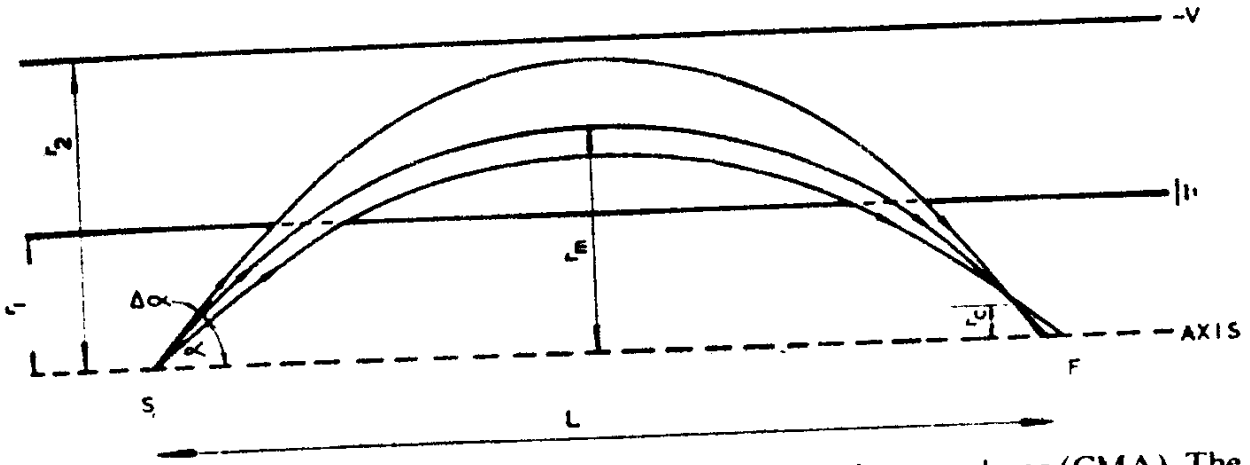

Figure 2.22 Diagrammatic arrangement of a cylindrical mirror analyser (CMA). The radii are r_1 for the inner cylinder and r_2 for the outer cylinder. The inner cylinder is earthed and a potential $-V$ is applied to the outer cylinder. Electrons emitted from a source S on the axis with a kinetic energy E_o are re-focused at F according to the expression (2.10). The entrance angle α is chosen to be 42° 18′, since at that angle the CMA becomes a second-order focusing device. A typical angular aperture $\Delta\alpha$ would be 6°. L is the distance between S and F, r_c is the position of the minimum trace width and r_m the maximum distance off the axis for electrons entering the analyser at 42° 18′. (After Bishop, Coad and Rivière[36])

$$E_o/eV = k/\ln(r_2/r_1) \quad mv^2/r = eV$$

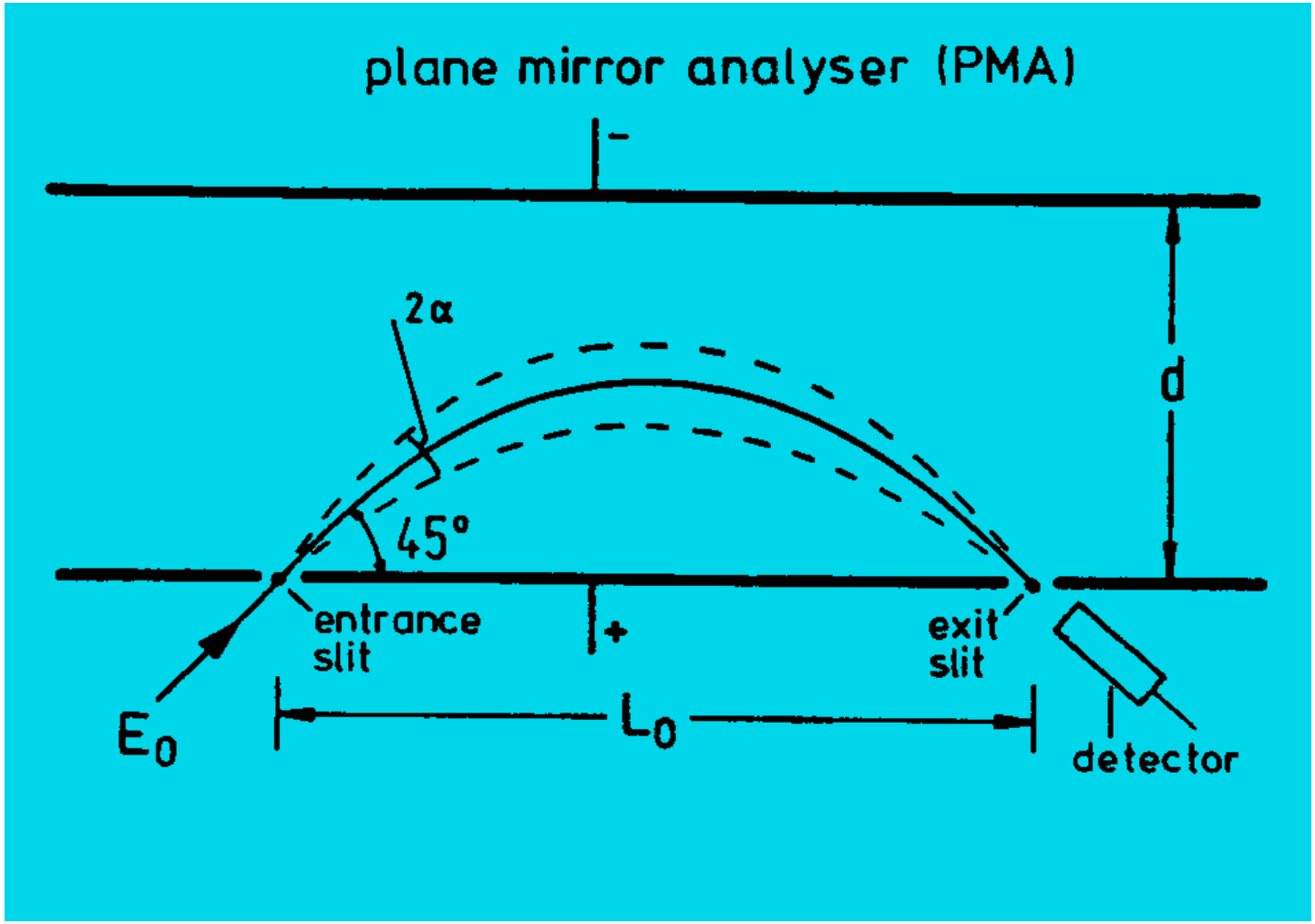
plane mirror analyser (PMA)
-
2α
d
45°
entrance
slit
+
exit
slit
E0
L0
detector

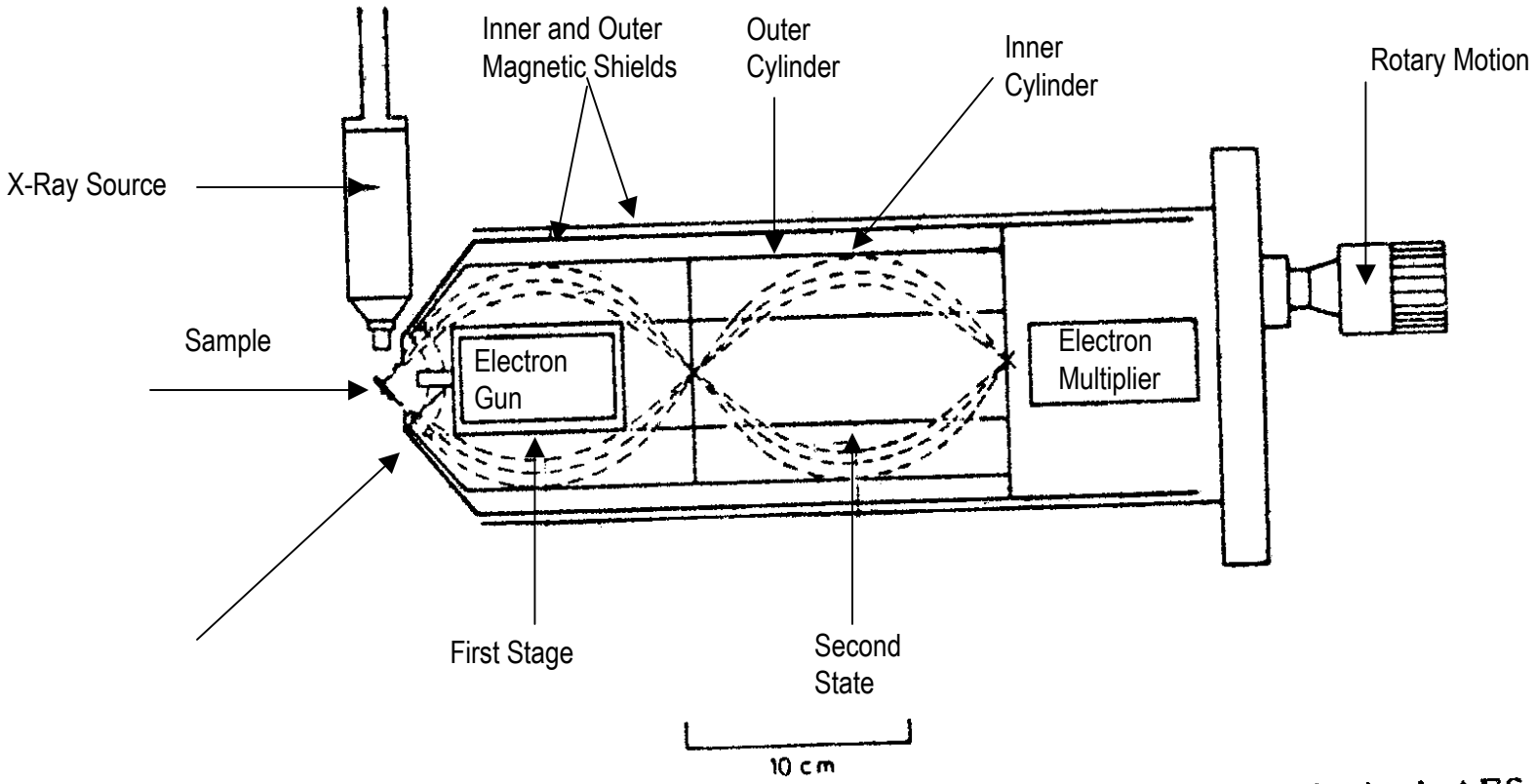

Figure 2.23 Diagrammatic arrangement of a double-pass CMA, used for both AES and XPS. The exit aperture from the first stage is the entrance aperture to the second stage. At the front end of the analyser are two spherical retarding grids centred on the source area of the sample that retard photo-electrons to a constant pass energy for XPS, For AES the grids are at earth potential, as is the inner cylinder. An externally operated rotary motion allows the entrance and exit apertures to the second stage to be changed remotely, from large sizes for XPS to small sizes for AES. The electron gun is situated on the axis of the CMA internally, but the X-ray source, of the type seen in detail in Figure 2.9(a), is external and positioned as close to the sample as the geometry will allow. (Reproduced from Palmberg[40] by permission of Elsevier Scientific Publishing Company)

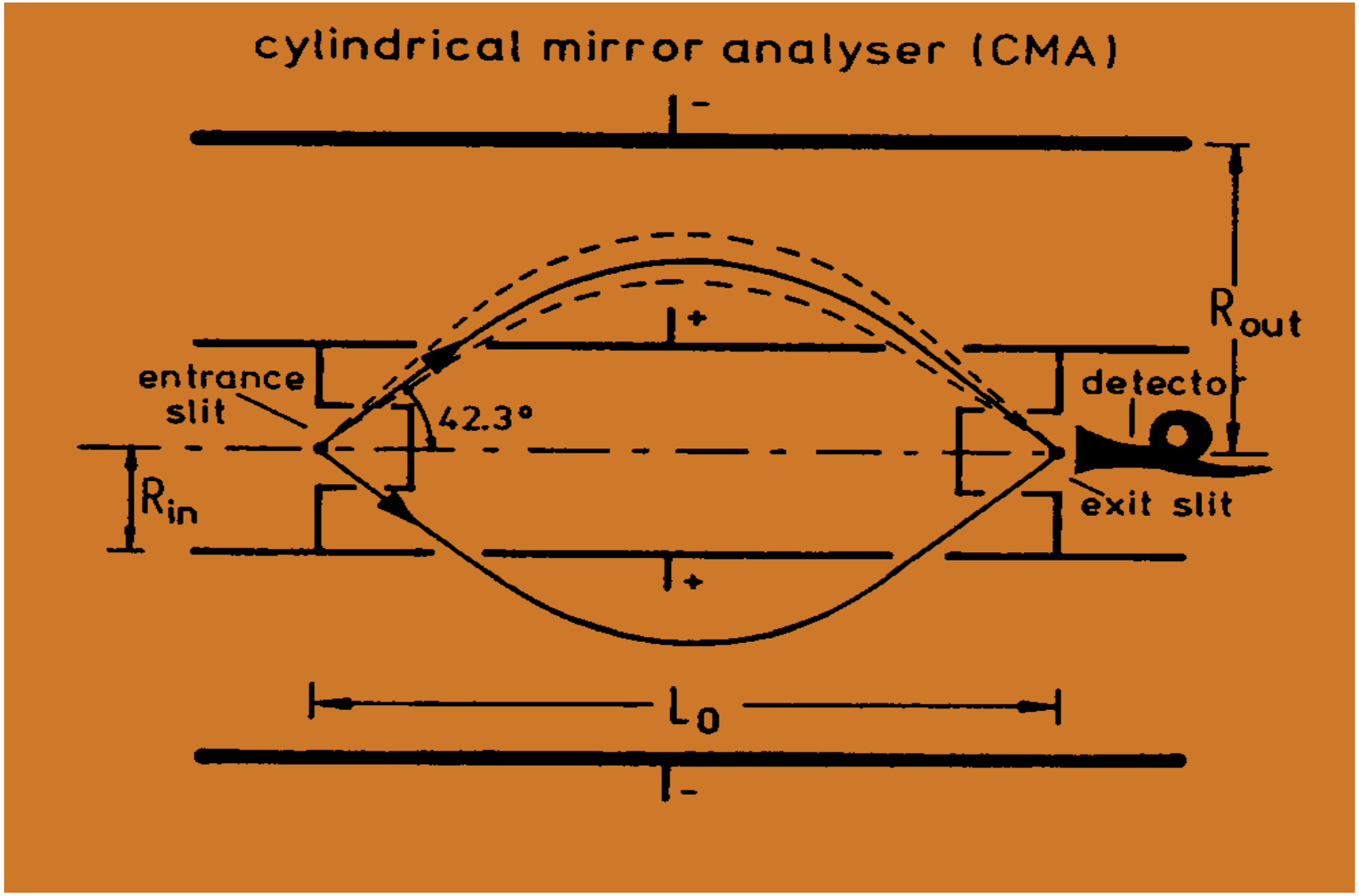
cylindrical mirror analyser (CMA)
-
+
+
-
R_{out}
R_{in}
entrance slit
42.3°
detecto
exit slit
L_0

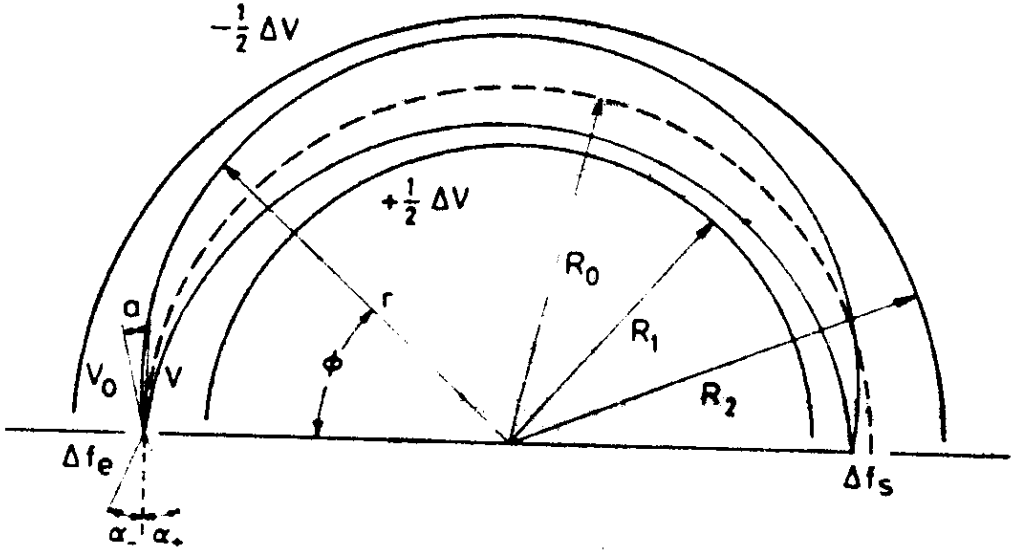

Figure 2.24 Principle of operation of the concentric hemispherical analyser. Two hemispherical surfaces of inner radius R_1 and outer radius R_2 are positioned concentrically. A potential ΔV is applied between the surfaces so that the outer is negative and the inner positive with respect to ΔV. R_0 is the median equipotential surface between the hemispheres, and the entrance and exit slits are both centred on R_0. If E is the kinetic energy of an electron travelling in an orbit of radius R_0, then the relationship between E and V is given by expression (2.21). ϕ and r are the angular and radial coordinates, respectively, of an electron of energy E_0 ($= e\Delta V_0$) entering the analyser at an angle α to the slit normal. If this electron is to pass through the exit slit, its path in the analyser is governed by the conditions of expression (2.22). (Reproduced from Roy and Carette[43] by permission of the National Research Council of Canada)

$$e\Delta V = E(R_2/R_1 - R_1/R_2)$$

cylindrical deflection analyser (CDA)

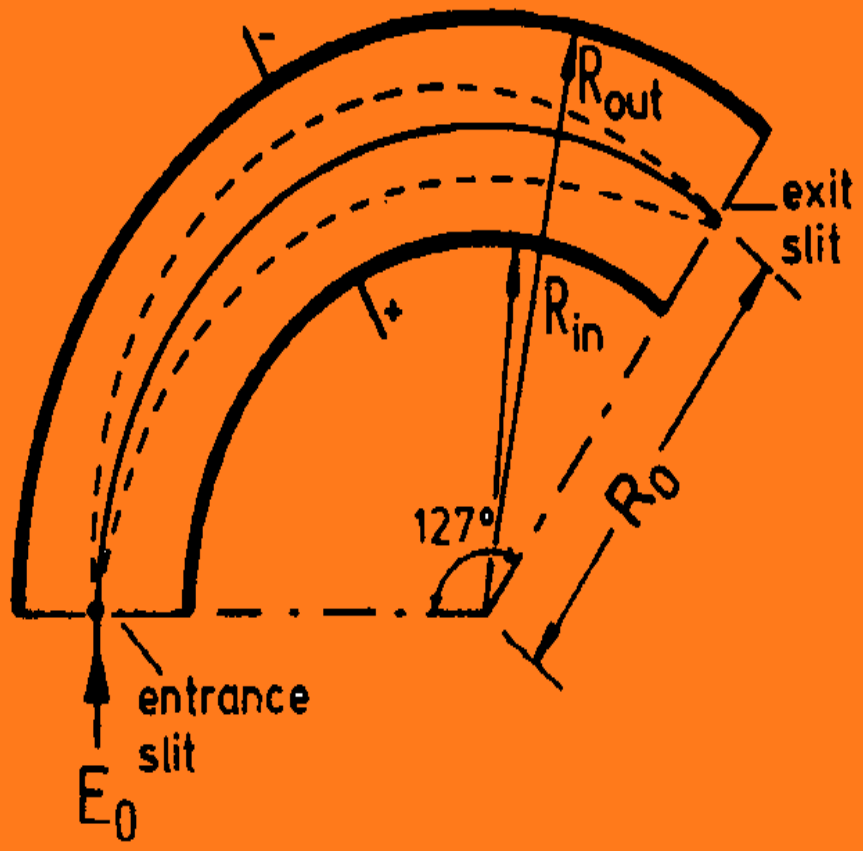

spherical deflection analyser (SDA)

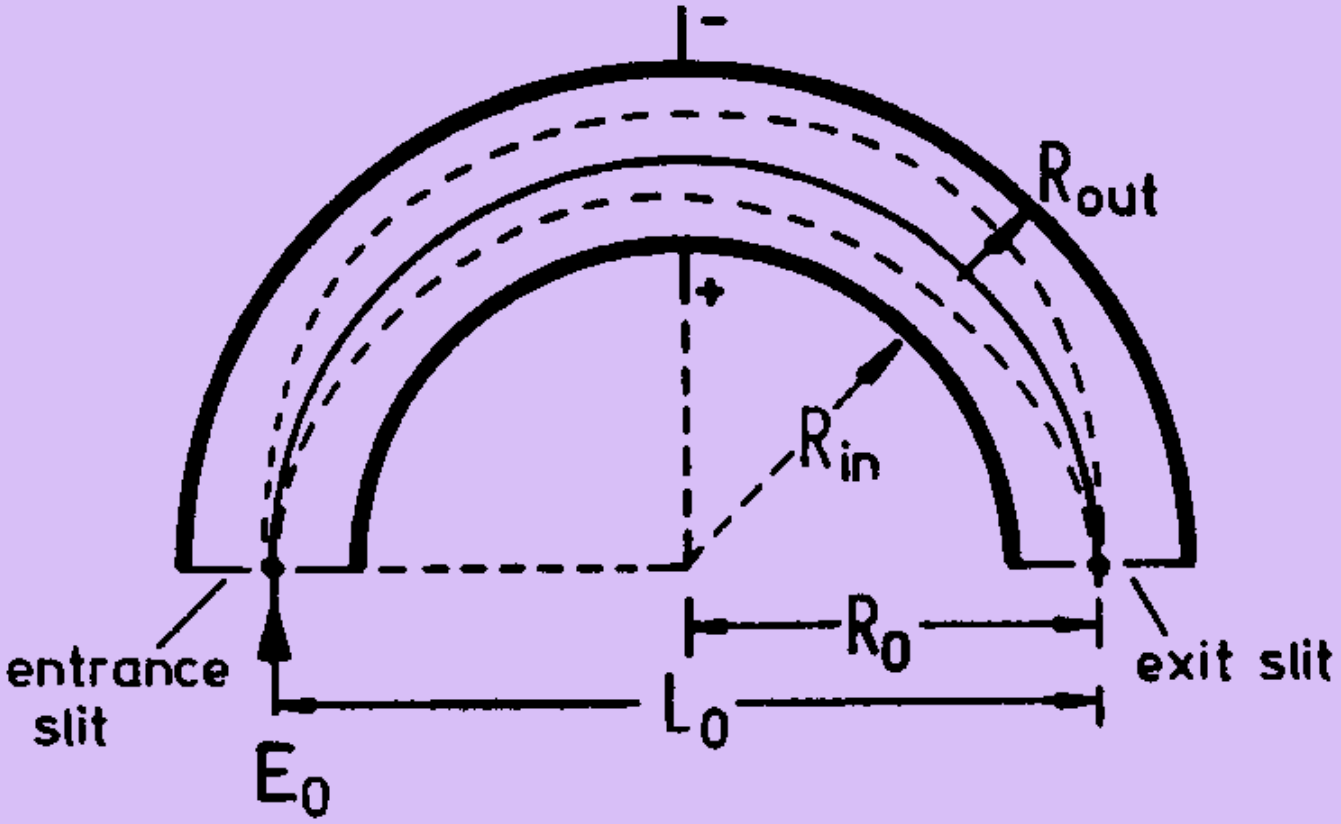

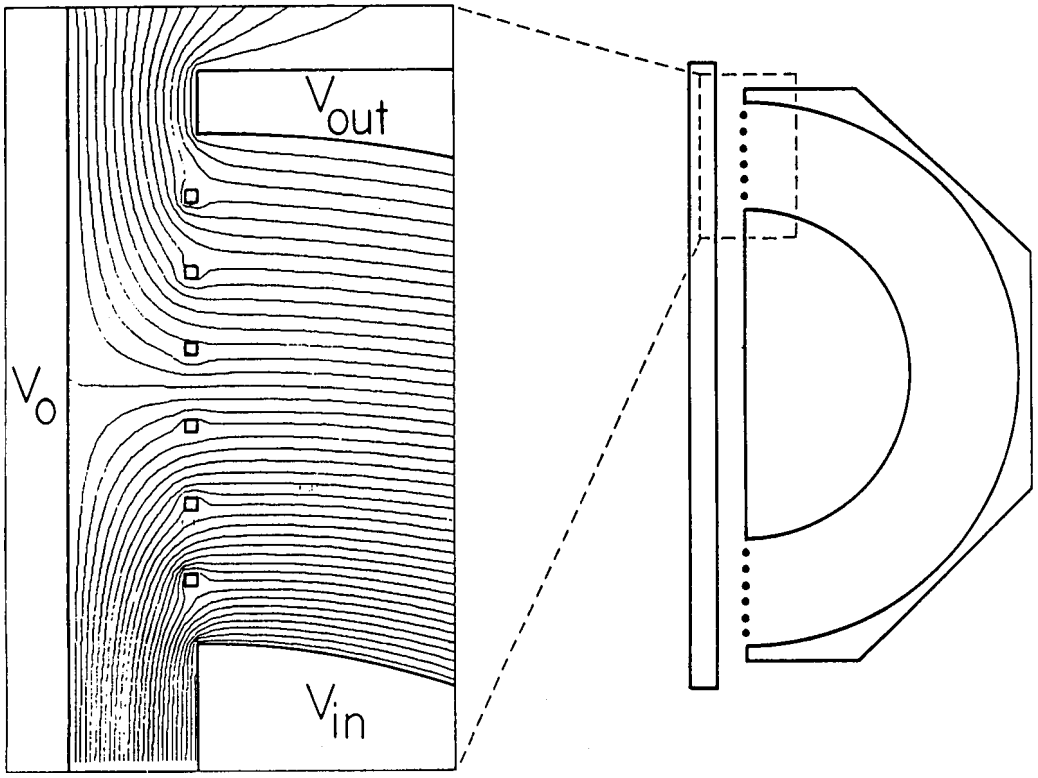
V_{out}
V_o
V_{in}

1. Single-Channel Detector

Channel electron multiplier:A continuous dynode surface. High count rate of 10^6 counts per second.

2. Multi-Channel Detector

A set of parallel detector chains or position sensitive detectors kept at the analyser exit slit plain.

Channel electron multiplier

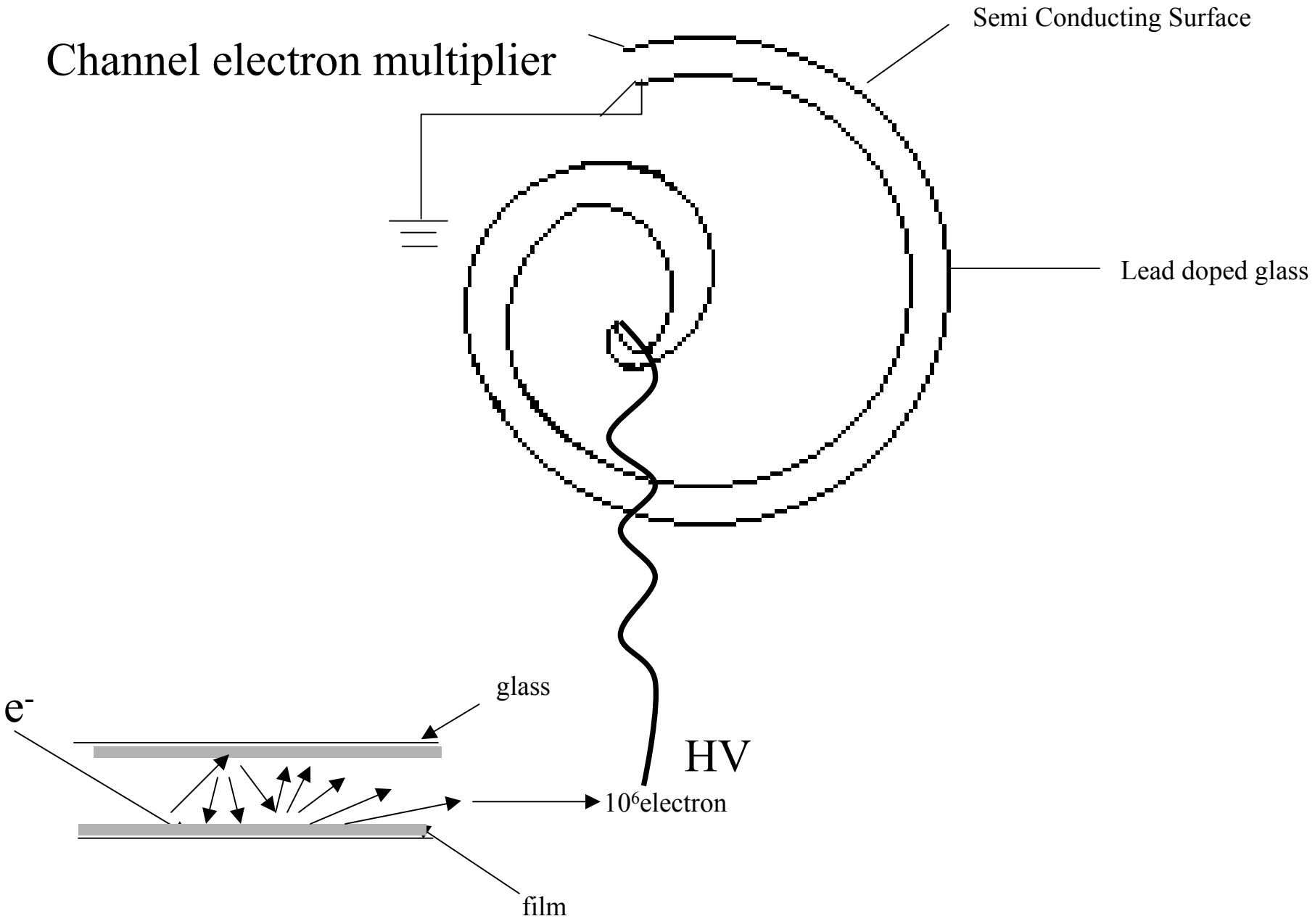

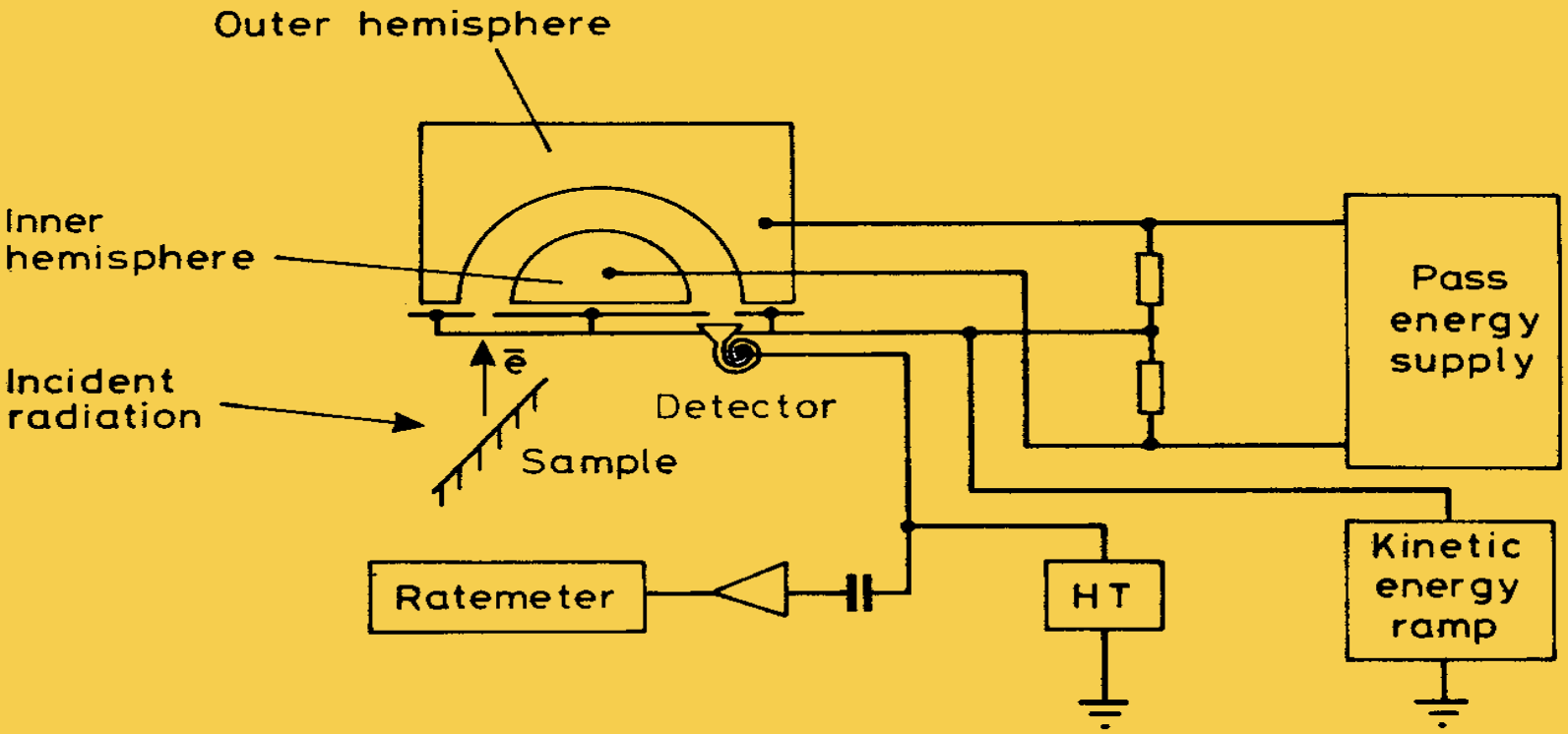

Hemispherical sector electron energy analyser and control electronics.

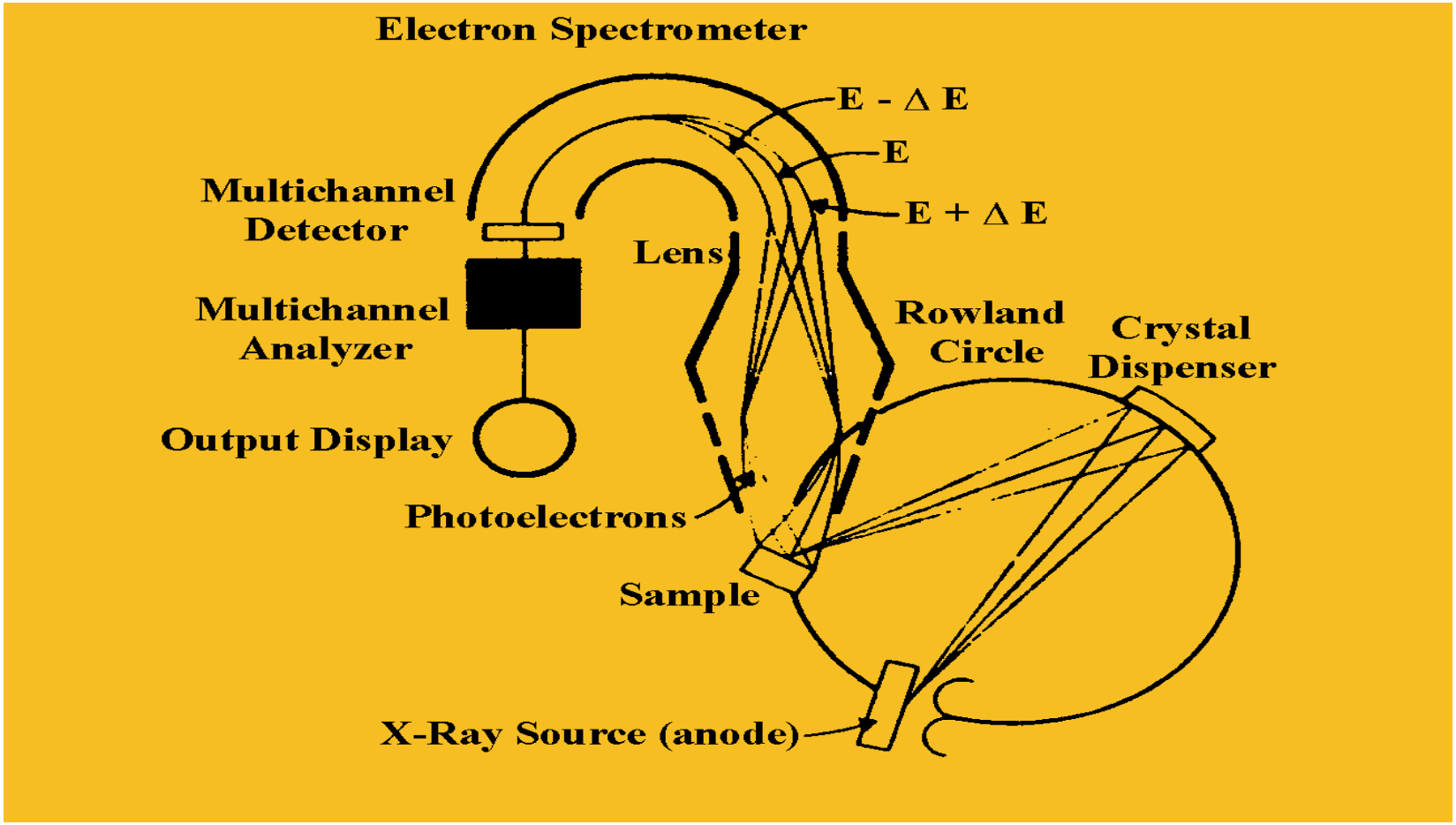

Spectrometer with X-ray monocromatisation

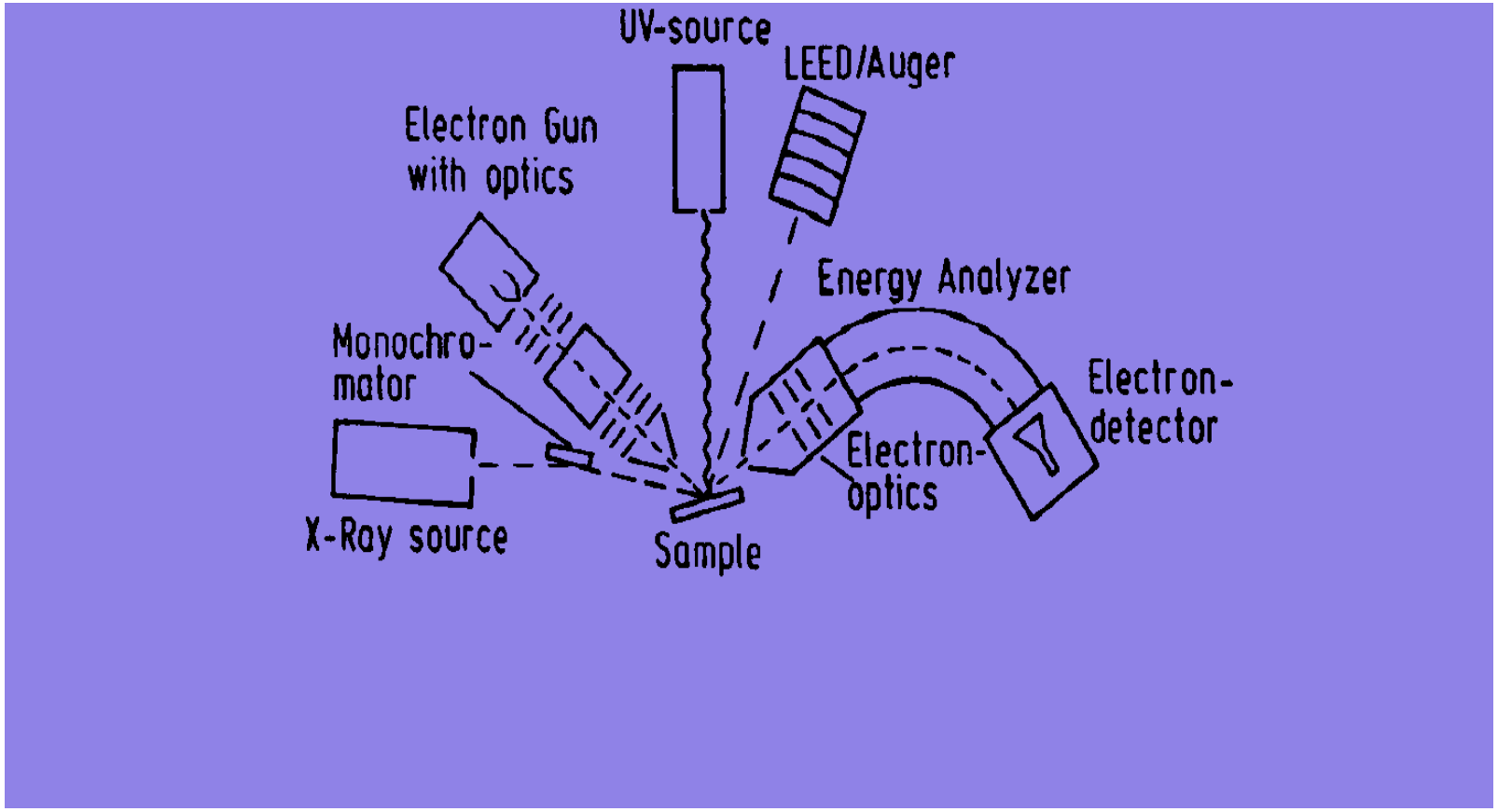

Modern instrument for UPS, XPS, AES and EELS

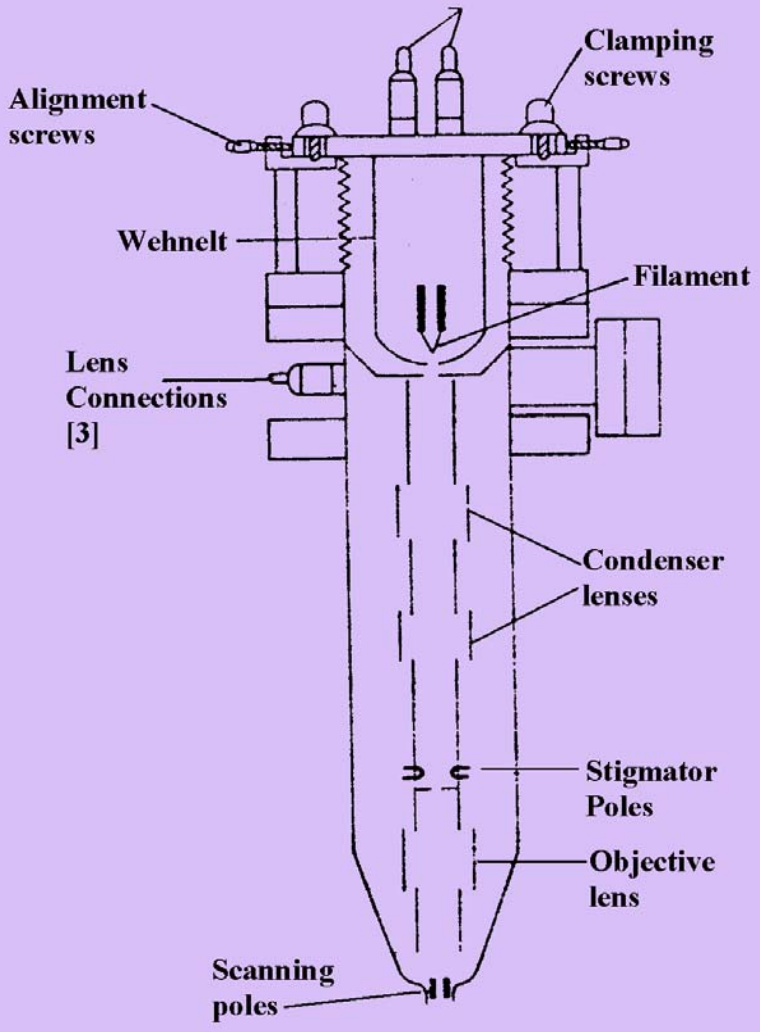

An electron gun for beams up to 10 ke V

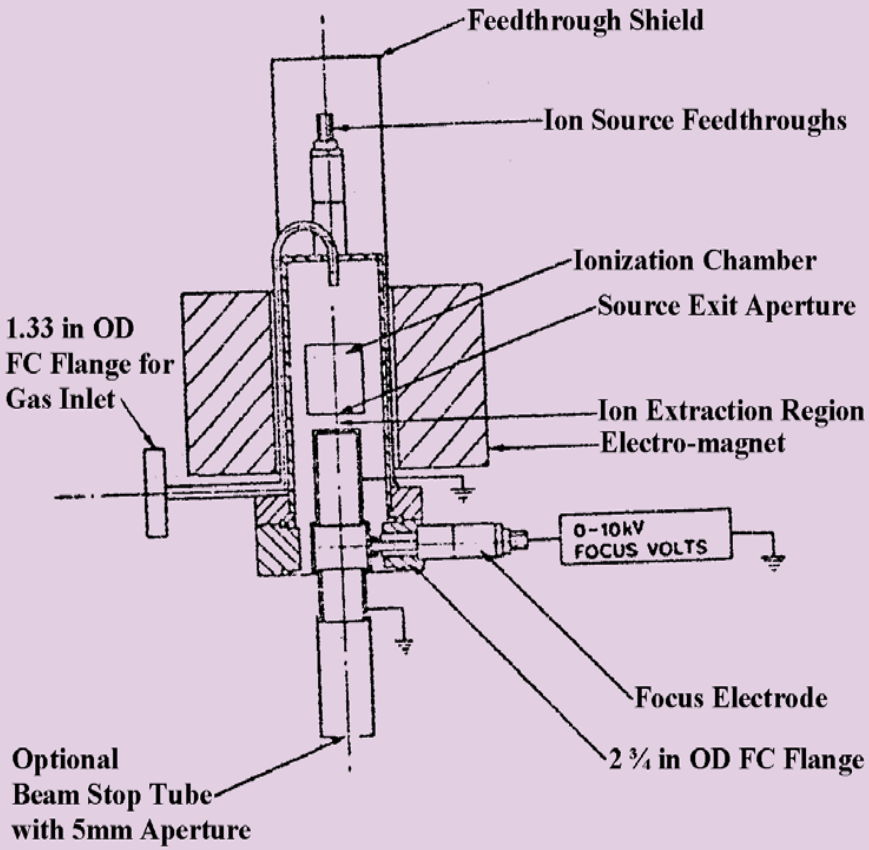

Ion gun using a Penning discharge.

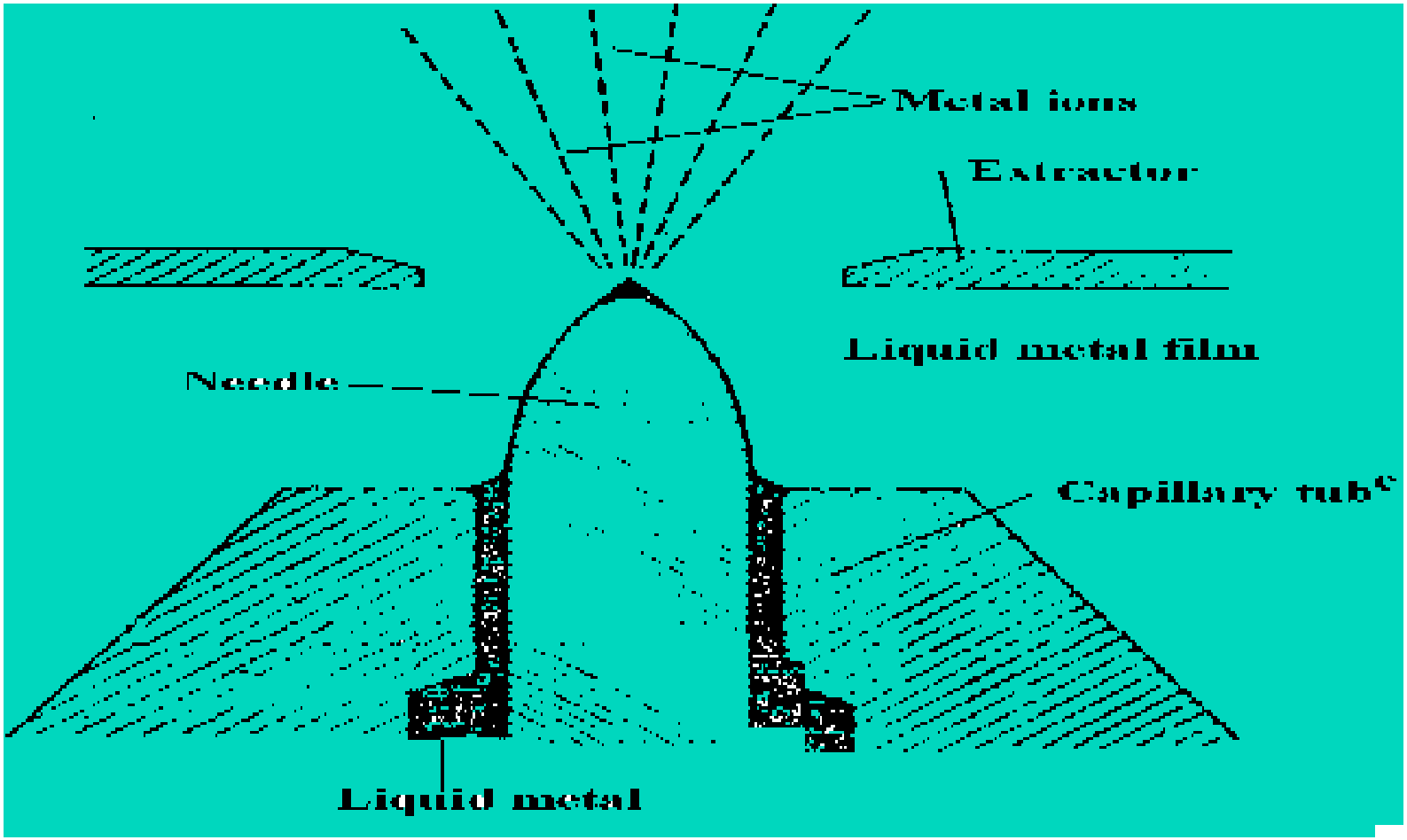

A liquid-metal field emission ion source

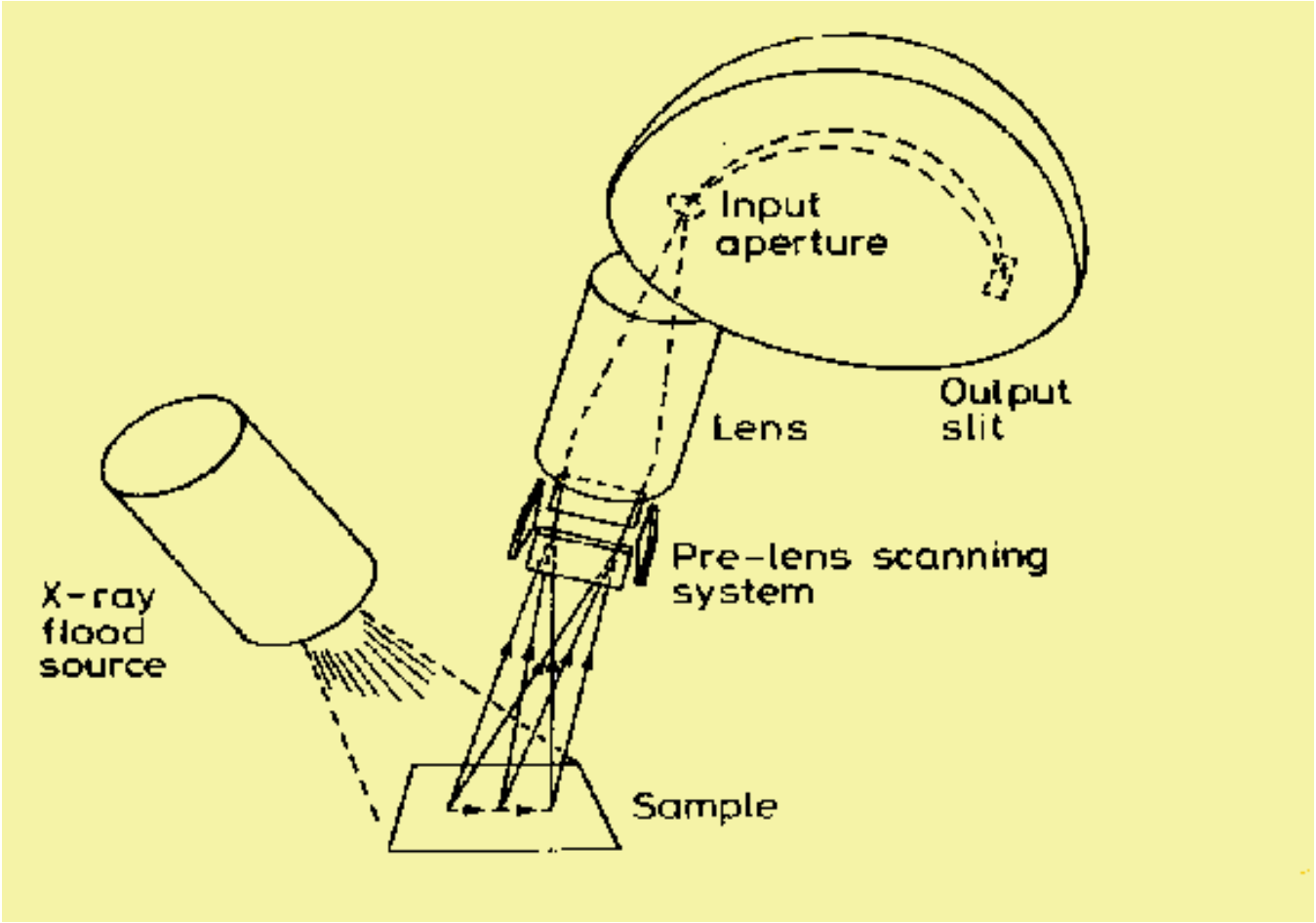

A simple method of XPS imaging using a conventional HAS instrument

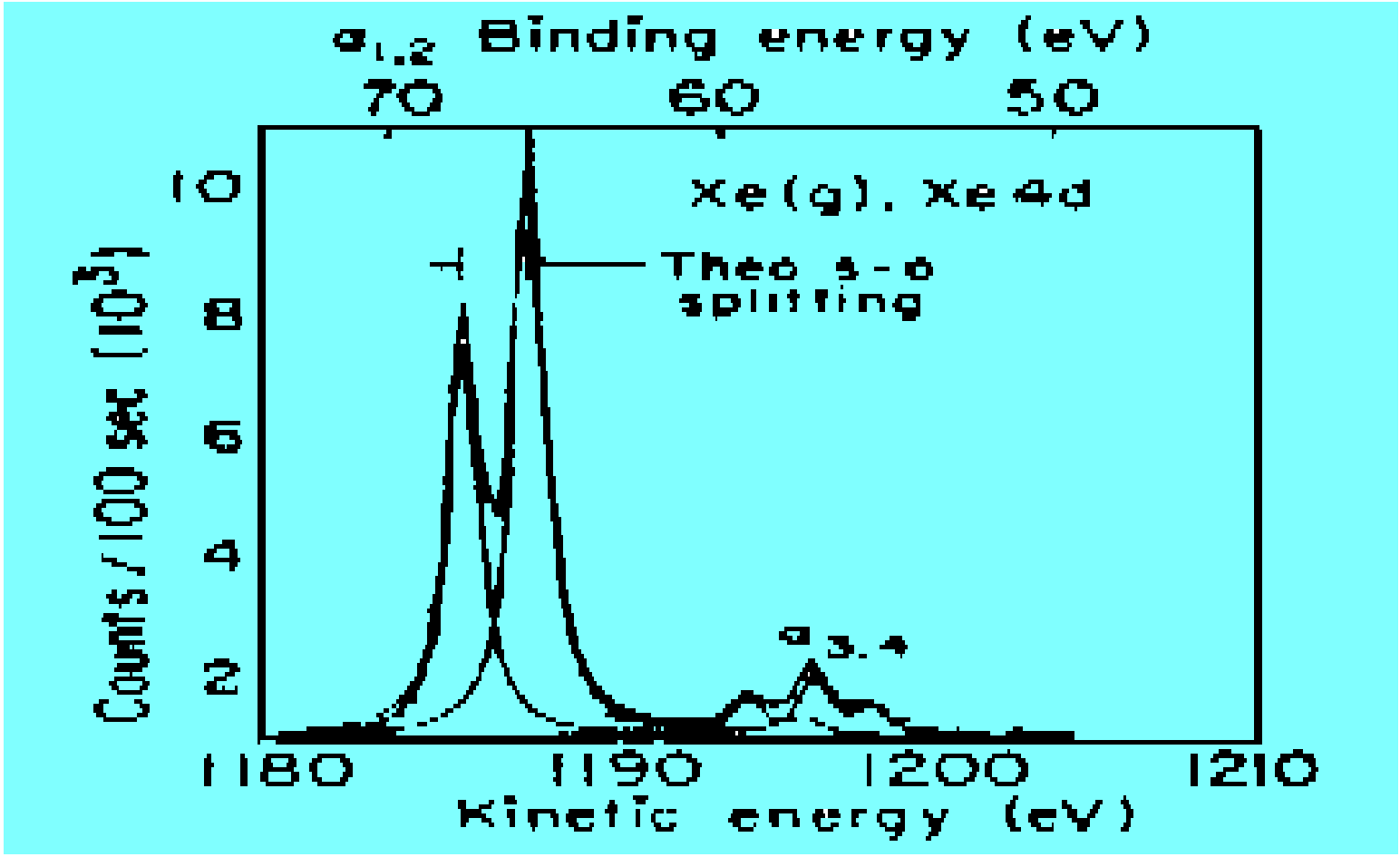

Data analysis